CHEMICAL ENGINEERING SCIENCE
GENIE CHIMIQUE

VOL. 4 JUNE 1955 No. 3

Thermal insulation of a raw sugar silo
Measurement by electrical analogue

S. HILL and E. G. MULLER
Tate & Lyle Research Laboratory, Keston, Kent

(*Received* 27 *November* 1954)

Summary—The electrical analogue method of investigating heat transfer processes was used to determine the thermal characteristics of proposed wall and roof structures for a 40,000 ton raw sugar silo. Thermal insulation is necessary to prevent internal temperature gradients and consequent transport of moisture. Simplification of the problem was achieved by separating the external temperature factors into a daily variation of air temperature, a seasonal variation and solar radiation. The details of the method are illustrated by calculating the constants of one of the analogue networks. Results for seven structures are tabulated.

Effective thermal conductivities of 19 packed raw sugars were measured to provide data not previously available. The conductivities are shown to be related to the moisture content and the bulk density of the packed sugar.

Résumé—Pour déterminer les caractéristiques, thermiques des murs et de la toiture d'un silo à sucre brut d'une capacité de 40.000 tonnes, les auteurs utilisent la méthode d'étude des processus de transfer de chaleur dite " méthode d'analogie électrique".

Une isolation thermique permet d'éviter des gradients de température interne et par conséquent le transport d'humidité. Le problème se simplifie en séparant les facteurs externes de la température en une variation journalière de la température de l'air, une variation saisonnière et une irradiation solaire.

Les auteurs illustrent les détails de la méthode par le calcul des constantes d'un des réseaux d'analogue. Ils donnent leurs résultats pour le calcul de sept constructions. Ils mesurent les conductivités thermiques effectives de dix-neuf empilements de sucre brut afin d'obtenir des données manquant jusqu'à présent. Ils montrent que les conductivités sont liées à l'humidité occluse et à la densité brute du sucre empilé.

INTRODUCTION

When raw sugar is stored in bulk there is a possibility of loss of sugar on account of the activity of micro-organisms (osmophilic yeasts and moulds) which increases with increasing moisture content. Raw sugar contains a small quantity of water, of the order of 0·5%. The percentage is variable but is usually less than the value at which appreciable destruction of sugar occurs. If temperature gradients were to arise within the sugar they would cause thermal transport of moisture towards the regions at the lower temperatures and the moisture content might be increased locally above the threshold value. Furthermore, the regions at the higher temperatures would be hardened by loss of moisture and difficulties would be experienced when the sugar was reclaimed from the silo.

A silo designed to hold 40,000 tons of raw sugar was recently built at the Plaistow Wharf (London) Refinery of Tate and Lyle Ltd. [1]. The silo has a retaining wall in the form of a vertical steel

cylinder of diameter 160 ft. and height 90 ft. and it is spanned by a slightly domed roof. Full capacity is achieved with a depth of sugar of 80 ft. The total exposed surface area of a solid circular cylinder of fixed volume resting on the ground with its axis vertical is a minimum when its height is equal to its radius. This condition is fulfilled by the cylinder of sugar at full capacity (height = radius = 80 ft.) but in spite of this the surface area amounts to 60,000 sq. ft. and the mass of sugar within 3 ft. of the surface is about 6,000 tons. The condition during storage of the sugar in this boundary layer is a matter of considerable importance.

Temperature gradients near to the surface of the sugar due to changes of ambient temperature must therefore be reduced by the provision of adequate thermal insulation of the walls and roof of the silo. Certain insulating systems were proposed and their thermal properties were investigated by means of the electrical analogue method [2, 3].

Theory of the Electrical Analogue

The distribution of temperature throughout a system of uniform, isotropic heat conducting media in contact with each other is determined at all points by Fourier's equation :

$$\frac{\partial^2 T}{\partial x^2} + \frac{\partial^2 T}{\partial y^2} + \frac{\partial^2 T}{\partial z^2} = \frac{\rho c}{k} \cdot \frac{\partial T}{\partial t}$$

$$\text{or} \quad \nabla^2 T = \frac{1}{\alpha} \cdot \frac{\partial T}{\partial t} \qquad (1)$$

Similarly the distribution of potential in an electrically conducting system is determined by an analogous equation :

$$\nabla^2 V = R C \cdot \frac{\partial V}{\partial t} \qquad (2)$$

in which R is the resistivity and C is the capacitance per unit volume.

ρ, c and k in the thermal case, and R and C in the electrical case are constant within each region of the system but vary from one region to another.

The electrical analogue method is based on the similarity of equations (1) and (2).

Analogous quantities are :

Temperature :	Voltage
Heat :	Electric charge
Flow of heat	Electric current
Time :	Time
Thermal resistance :	Electrical resistance
Thermal capacity :	Electrical capacitance

Between any points of the electrical analogue the values of electrical resistance and capacitance are made proportional to the values of their thermal counterparts between the corresponding points of the thermal system.

In order to make the construction of an analogue a practical proposition it is necessary to use lumped resistors and capacitors in place of the theoretically ideal distributed impedances. The analogue now consists of a two or three-dimensional network of resistors with capacitors connected between earth and the junction points of the resistors. Lawson and McGuire [4] have discussed the magnitude of the errors involved by this substitution. Actual physical dimensions of the analogue units are, of course, of no significance. Corresponding points of the thermal and electrical systems are determined by the resistances and capacitances between the points. An important advantage of the analogue method is the reduction of the time scale. Whereas the time constant of a section of the thermal system might be of the order of days, that of the corresponding section of the analogue may be reduced if necessary to the order of microseconds. Cathode ray tube display of the voltage variations is a convenient means of indication. Temperature variations at the boundary of the thermal system are simulated by voltage variations at the corresponding points of the analogue. These have a similar wave form but are accelerated with respect to the temperature variations by the appropriate time scale ratio. Generation of heat at a point in the thermal system and flow of heat into it from outside are simulated by flow of current, of the appropriate value, into the corresponding points of the analogue.

Application to the Silo Problem

The radii of curvature of the walls and roof of the silo are very large compared to the depth of

VOL. 4 1955

penetration of the temperature variations into the sugar, so that for the purposes of this problem the walls and roof can be considered to be plane. Heat flow in the sugar and in the insulating layers is normal to the surface and is one dimensional. Thus the electrical analogue becomes a single line of resistors with capacitors to earth (Fig. 1).

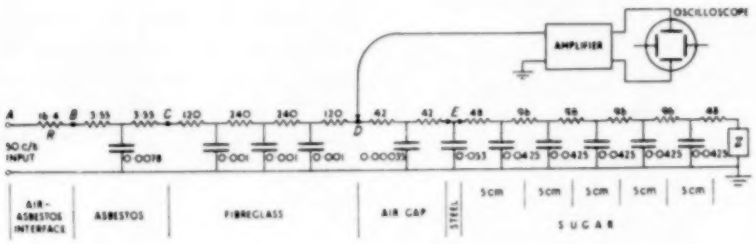

FIG. 1. Electrical analogue of the bottom of the silo wall, 1st design, for daily variations of air temperature. Resistances in thousands of ohms. Capacitances in microfarads. Z = characteristic impedance of the sugar sections.

To simplify the problem the three sources of temperature variation were considered separately. The sources are :

1. Daily variations of temperature of the air outside the silo,
2. Seasonal variations of temperature of the air outside the silo,
3. Solar radiation.

Since rate of heat transfer is proportional to the first power of temperature difference the effects of these three factors can be measured separately and added together. This is only approximately true for transfer across an air gap. Each of the six silo wall structures that were investigated included an air gap, but, as the temperature differences across the gaps are small, the approximation was considered to be sufficiently accurate.

Records show that in London the difference between maximum and minimum temperatures within a 24-hour period is not usually greater than 14°C and that this is also the difference between average July and January temperatures. The daily and seasonal variations can be treated with sufficient accuracy as sine waves of amplitude 7°C. The harmonics are small and have less penetrating power than the fundamentals on account of their higher frequencies. This approximation is justified by the oscillograms shown in Fig. 5. Both variations were represented at the input to the analogue by a 50 cycle/sec. voltage from the A.C. mains, so that two analogues, each with its appropriate time constants, were required for each insulating system. The analogue of solar radiation is a current flowing into the input end of the electrical line having a wave form corresponding to the daily variation of the flux of solar radiation. The form of this variation changes throughout the year, and the most severe conditions should be investigated if possible. On the roof most severe conditions occur on a cloudless day in midsummer. Consideration of the variation of severity of conditions affecting the wall is very complex. It was considered sufficient to investigate midsummer conditions for the south facing part of the wall.

It is shown in Appendix 2 that, in midsummer at latitude ψ, the intensities of radiation on a horizontal surface (roof) and on the south facing part of the silo wall are respectively :

$$N_R = N_0 (0{\cdot}92 \cos \psi \sin \omega t + 0{\cdot}40 \sin \psi)$$

and

$$N_W = N_0 (0{\cdot}92 \sin \psi \cos \omega t + 0{\cdot}40 \cos \psi)$$

These expressions are applicable when they are positive. Negative values of N_R mean that the intensity is zero as the sun is below the horizon.

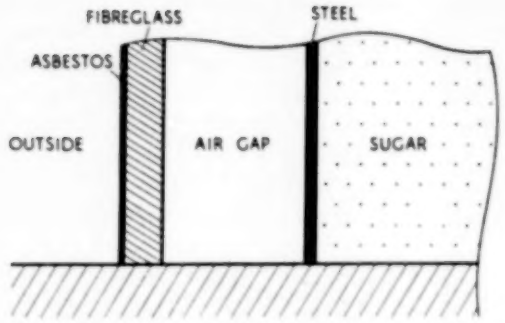

Fig. 2. Section through the bottom of the silo wall, 1st design.

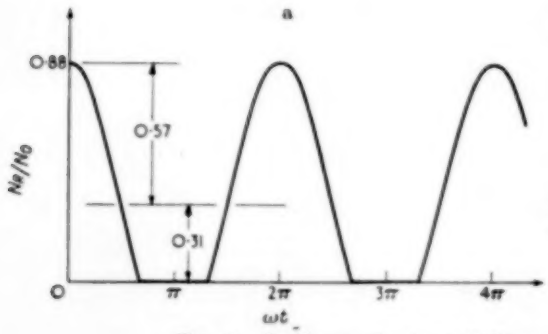

Fig. 3. Incidence of solar radiation. (a) on the roof; (b) on the south wall.

When N_W is negative the sun is behind the plane of a south facing wall.

London is at latitude $\phi = 51\frac{1}{2}°$ so that

$$N_R = N_0 (0{\cdot}57 \cos \omega t + 0{\cdot}31)$$

and

$$N_W = N_0 (0{\cdot}72 \cos \omega t - 0{\cdot}25)$$

These wave forms are shown in Fig. 3 (a and b). Interrupted cosine current waves required to satisfy the expressions for N_R and N_W were produced by means of the circuit shown in Fig. 4, in which the valve is biassed so that the correct proportion of the full wave is suppressed. Fig. 5(a) shows an oscillogram of the input current wave form.

The effects of the three sources of temperature variation could have been obtained by direct calculation but the calculation would have involved the lengthy solution of sets of simultaneous equations derived from the boundary conditions at each of the interfaces between the layers. In addition it would have been necessary to resolve the non-sinusoidal effect of solar radiation into its Fourier components and solve the equations for each component separately. Furthermore each of the systems investigated would have required a complete calculation, whereas the analogues were assembled and measured in a short time.

Calculation of the Constants of an Analogue

The procedure for detailed calculation of an analogue will now be illustrated by reference to the "daily" analogue of one of the systems proposed for the silo wall. The layer of steel which bears the lateral thrust of the sugar tapers from

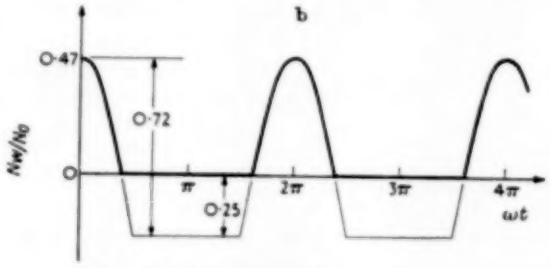

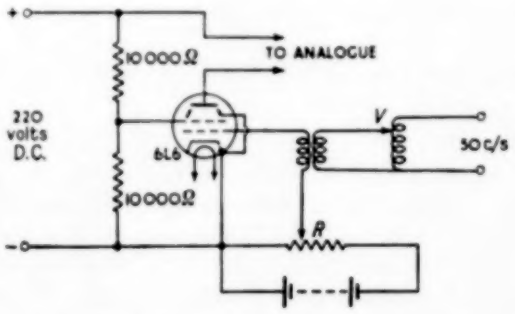

Fig. 4. Circuit for interrupted cosine waves of current.

bottom to top. The analogue given here represents the bottom of the wall where the thickness of the shell is greatest. A full specification of the bottom of the wall is given in Table 1 below.

For the purpose of heat transmission the wall consists of the five layers indicated in Fig. 2, which is not to scale. Their relevant properties, together with those of an average raw sugar are :

VOL. 4 1955

Table 1.

1. Material		*Air asbestos interface*	*Asbestos*	*Fibre-glass*	*Air gap*	*Steel*	*Sugar*
2. Thickness (metres)	d	0	0·00635	0·0762	0·381	0·0203	
3. Density (kg/metre^3)	ρ	–	1762	80	1·22	7800	910
4. Mass/metre^2 (kg/metre^2)	m $(= \rho \times d)$	–	11·2	6·1	0·46	158	910/ metre depth
5. Sp. Ht. (joules/kg °C)	c	–	922	658	1006	448	1250
6. Thermal Conductivity (watts/metre °C)	k	–	0·28	0·033	–	45	0·161
7. Thermal Resistance per metre^2 (°C/watt)	R_t $(= d/k)$	0·053	0·023	2·3	0·26	0·00045	6·2/ metre depth
8. Thermal Capacity per metre^2 (joules/°C)	C_t $(= c \times m)$	0	10350	4000	463	70800	$1{\cdot}14 \times 10^6$/ metre depth
9. Time Constant (seconds)	τ $(= R_t \times C_t)$	0	238	9300	123	30	$7{\cdot}1 \times 10^6$/ metre^2

Note : 1 day = 86,400 seconds.

The thermal resistances of the air-solid interface and the air gap were taken from *The Computation of Heat Requirements for Buildings*, published by the Institution of Heating and Ventilating Engineers, 1950.

In row 9 of Table 1 the "time constant" is the product of the thermal resistance and thermal capacity of a square metre of the particular layer considered. It has the dimensions of time only and is independent of the cross sectional area.

Let us select any one of the layers that has both resistance and capacity – say the fibreglass. We must satisfy the condition :

$$\frac{\text{Time constant of the fibreglass section of the analogue}}{\text{Time scale of the electrical signal}} = \frac{\text{Time constant of the fibreglass}}{\text{Time scale of the temperature variation}}$$

$$= \frac{9{,}300 \text{ seconds}}{86{,}400 \text{ seconds}} = 0{\cdot}108$$

The period of the electrical signal from the mains is 0·02 seconds. Hence the time constant of the fibreglass section

$$= 0{\cdot}108 \times 0{\cdot}02 \text{ secs.} = 2{\cdot}16 \times 10^{-3} \text{ secs.}$$

We may now arbitrarily set the capacitance of the fibreglass section to some convenient value – say 0·003 microfarads – and enter this value* in row 3 of Table 2.

Then since $RC = 2{\cdot}16 \times 10^{-3}$ secs.

$$R = \frac{2{\cdot}16 \times 10^{-3}}{3 \times 10^{-9}} = 7{\cdot}2 \times 10^5 \text{ ohms}$$

This value† is entered in row 2 of Table 2. The other sections of the analogue are given resistances and capacitances which are proportional to their thermal resistances and capacities, the values being based on 0·003 μ farads and $7{\cdot}2 \times 10^5$ ohms for the fibreglass section.

Experimental Procedure

(a) *Daily and Seasonal Temperature Variations*

Each of the analogues was assembled as shown in Fig. 1. The amplifier of the cathode ray oscillograph was connected between earth and a probe

Table 2.

1. Material		*Air asbestos interface*	*Asbestos*	*Fibre-glass*	*Air gap*	*Steel*	*Sugar*
2. Electrical Resistance (ohms)	*R*	16400	7100	720000†	84000	140	19200/cm depth
3. Electrical Capacitance (μ farads)	*C*	0	0·0078	0·0030*	0·00035	0·053	0·0085/cm depth

Ideally the network should be terminated as shown by an impedance equal to the characteristic impedance of the sugar sections, but this termination was not actually used as the amplitude of the signal was reduced almost to zero at the fifth sugar section so that spurious reflections were negligible.

In the "seasonal" analogue each of the five sugar sections represented a 100 cm depth of sugar.

Table 3.

Structure	*Materials*	*Thickness of layer (cm)*	*Insulation factor*	
			Daily	*Seasonal*
Top of wall (1st design)	Asbestos Fibreglass Air gap Steel	0·635 7·62 38·1 0·38	14	1·5
Bottom of wall (1st design)	Asbestos Fibreglass Air gap Steel	0·635 7·62 38·1 2·03	29	1·5
Top of wall (2nd design)	Asbestos Air gap Steel	0·635 45·7 0·38	2·1	1·0
Bottom of wall (2nd design)	Asbestos Air gap Steel	0·635 45·7 2·03	3·0	1·0
Roof 1	Foam concrete	8·9	5·0	1·15
Roof 2	Ruberoid Steel	0·635 0·317	2·1	1·0
Top of wall of Swedish silo	Steel Air gap Wood	0·38 15·2 3·81	4·6	1·1
Bottom of wall of Swedish silo	Steel Air gap Wood	2·03 15·2 3·81	4·6	1·1

Design 2 differs from design 1 in that it has no fibreglass. An air space 6 metres thick was assumed to exist below the roof.

The Swedish silo above represents an existing structure at Gothenburg and is included here for comparison.

VOL. 4 1955

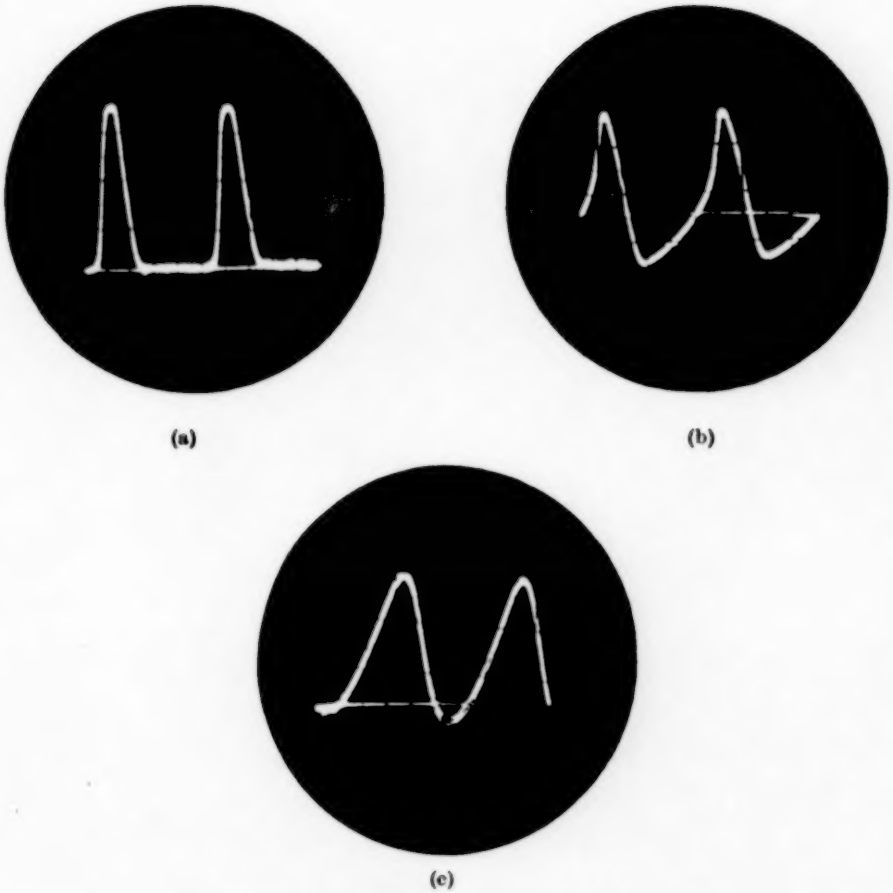

FIG. 5. Temperature wave forms due to solar radiation. (a) at the outer surface of the asbestos (*B*); (b) at the outer surface of the sugar (*E*); (c) 12·5 cm inside the sugar (*F*). Refer to Fig. 1 for points *B*, *E* and *F*.

which could be applied to each of the points *A*, *B*, *C* . . . Having set the input voltage and the amplifier gain to give a predetermined amplitude on the oscillograph screen with the probe at the point *A*, the probe was applied to the points *B*, *C*, *D* . . . and the amplitudes were observed. The effectiveness of the thermal insulation is given by an " insulation factor " which is defined as the ratio of the amplitudes at the points *A* and *E* of the system. At any of the internal points *B*, *C*, *D* . . . the phase of the signal is changed with respect to the input signal. This phase change can be readily observed if the horizontal sweep of the oscillograph is locked directly with the 50 cycle/sec. supply (Fig. 5).

(b) *Solar Radiation*

Having decided, arbitrarily, the relation between voltage and temperature the current required to represent a given flux of radiation can be calculated by noting that the dimensionless quantities :

$$\frac{\text{Temperature} \times \text{Capacity/unit area}}{\text{Time scale} \times \text{Heat flux/unit area}}$$

and

$$\frac{\text{Voltage} \times \text{Capacitance}}{\text{Time scale} \times \text{Current}}$$

are equal.

Heat transferred from the surface to the atmosphere by conduction and convection must be allowed for by connecting the resistance *R* of Fig. 1, the analogue of the surface film resistance, from the point *B* to earth. When measuring the effect of radiation on the south wall *R* was increased by a factor 5/3 to take account of the fact that the surface resistance of a south wall is 5/3 times the average for the wall as a whole. For the roof the surface film resistance was taken as half of that for a south wall. A current, adjusted to the correct wave form by the setting of *R* and *V* in the circuit of Fig. 4 is fed in at *B*.

As the input is not now sinusoidal the wave form of the voltage-time curve changes from point to point of the network. Oscillograms (which are relatively not to scale) of some of the wave forms are shown in Fig. 5. It can be seen that

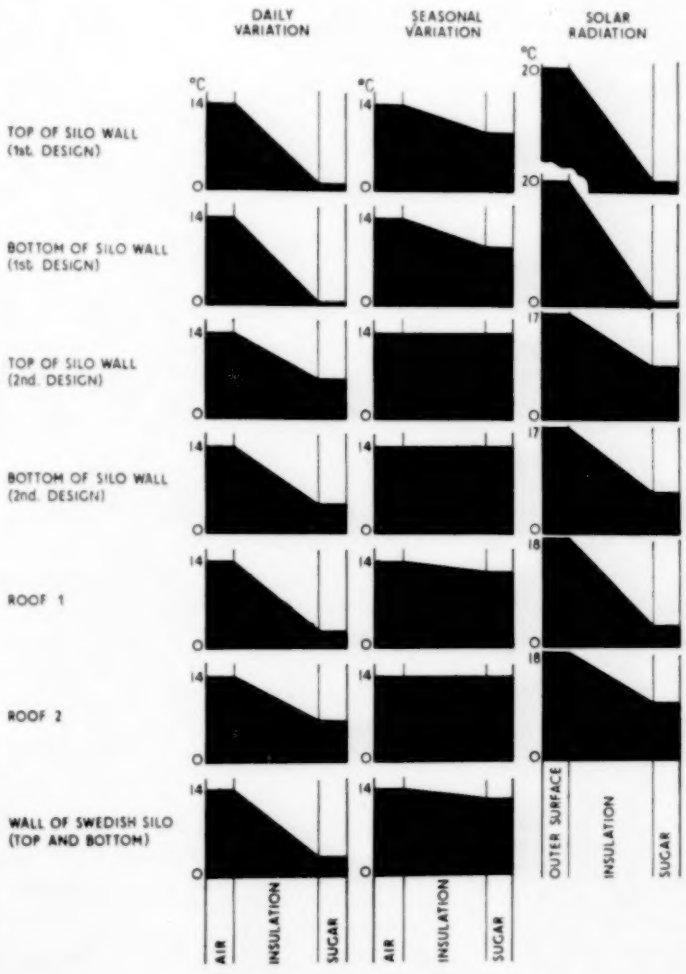

Fig. 6. Temperature ranges (range = 2 × amplitude).

Column 1. Due to daily temperature variation.
Column 2. Due to seasonal temperature variation.
Column 3. Due to solar radiation in midsummer.

The height of the left hand side of a shaded area represents the range of temperature at the outer surface of the wall or roof ; the height at the right hand side represents the range at the surface of the sugar.

the wave form becomes more nearly sinusoidal as it penetrates more deeply into the system.

Numerical Results

Details of the proposed wall and roof structures which were investigated are given in Table 3, in which the first mentioned layers are on the outside. Insulation factors are given in columns 4 and 5.

The insulation factors are illustrated graphically in Fig. 6. The heights of the left and right hand side of a shaded area indicate the ranges of temperature at the outer surface of the wall and the boundary of the sugar respectively. An absorption coefficient of 0·5 has been assumed for the calculation of the effective flux of solar radiation. The solar radiation diagrams represent midsummer conditions.

Two points of general interest can be noted.

(1) In all cases insulation is much less effective in suppressing the effect of the seasonal variation of temperature than in suppressing the daily variation. This is due to the effect of thermal capacity.

(2) The two silo walls (1st and 2nd designs) have greater insulation factors at the bottom than at the top. This is due to the difference between the thermal capacities per unit area of the steel shell at the top, where the thickness is 0·38 cm, and at the bottom, where the thickness is 2·03 cm. The steel has no appreciable thermal resistance, even at its thickest part.

APPENDIX I

As data on the effective thermal conductivities of raw sugars when packed under normal compressions were not available, measurements were made on nineteen raw sugars. Percentage moisture and bulk density were also observed.

Results are shown in Table 4.

For the purpose of designing the analogues, values of

$$k = 0{\cdot}161 \text{ watts/metre °C}$$

and $$\rho = 0{\cdot}910 \text{ kg/litre}$$

were taken as representative of an average raw sugar.

It is reasonable to suppose that the conductivity increases with moisture and with bulk density. If we assume a linear dependence of conductivity on moisture and density the regression equation is :

$$k = 0{\cdot}0527\,W + 0{\cdot}370\,\rho - 0{\cdot}1925$$

This equation holds within the limits :

$$0{\cdot}14 < W < 0{\cdot}85 \text{ and } 0{\cdot}825 < \rho < 0{\cdot}970$$

Statistical analysis shows that the coefficients of W and ρ are both significant. The standard deviation of the measured values of k from the values given by the equation is 0·0086, giving a coefficient of variation of 5%.

Consider a raw sugar having moitsure W%. If its moisture had been the average value $\overline{W}$ the conductivity, according to the equation, would have been 0·0527 $(W - \overline{W})$ less than the observed value. If we adjust all of the conductivities in this way we have a set of conductivities corrected for non-average moisture which we can plot, as in Fig. 7 (*a*) against bulk density.

In Fig. 7 (b) the conductivities, adjusted for non-average density, are plotted against moisture.

In both cases the correlation is good.

Table 4.

Origin of raw sugar	*Moisture* (%)	*Density* (*kg/litre*)	*Conductivity* (*watts/metre °C.*)
British West Indies	0·85	0·903	0·190
	0·64	0·910	0·182
	0·66	0·857	0·265
San Domingo	0·59	0·940	0·188
	0·50	0·860	0·157
	0·50	0·936	0·174
	0·53	0·879	0·155
Australia	0·14	0·939	0·154
	0·14	0·967	0·171
	0·14	0·885	0·142
Mauritius	0·23	0·879	0·143
	0·14	0·928	0·169
	0·15	0·904	0·156
England (beet sugar)	0·65	0·874	0·165
	0·61	0·949	0·193
	0·42	0·899	0·173
Cuba	0·49	0·910	0·160
	0·51	0·887	0·152
	0·45	0·825	0·131
Average	0·439	0·9016	0·1642

VOL. 4 1955

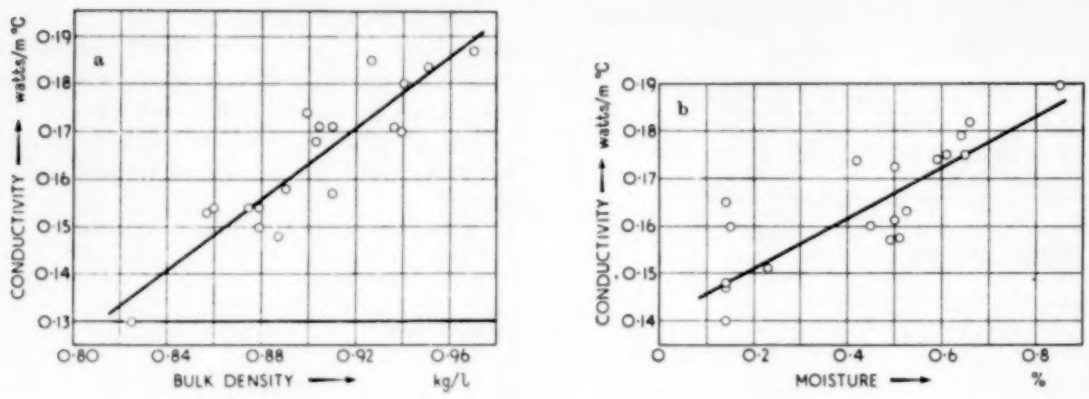

(a) (b)

FIG. 7. Thermal conductivities of raw sugar in bulk.

(a) Conductivity adjusted for non-average moisture plotted against bulk density. (b) Conductivity adjusted for nonaverage density plotted against moisture.

APPENDIX II

Calculation of the sun's elevation

Take the rectangular axes *Ox*, *Oy*, and *Oz* fixed in the earth and rotating with it (Fig. 8).

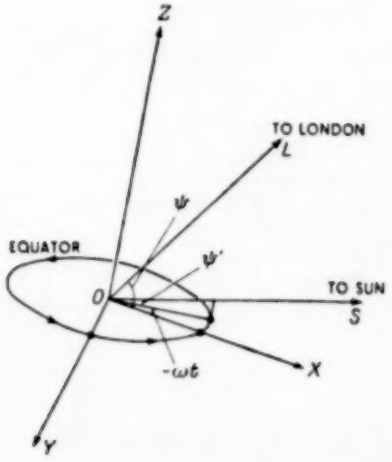

FIG. 8

Ox and *Oy* are in the equatorial plane.

Ox passes through the meridian of the locality in question, *Oz* is the polar axis. In midsummer the angle between *OS* and the *Oxy* plane $= \psi' = 23\frac{1}{2}°$.

The angle between *OL* and the *Oxy* plane $= \psi = 51\frac{1}{2}°$.

Let the direction cosines of *OS* be l_1, m_1, n_1 and of *OL* be l_2, m_2, n_2.

Then
$$l_1 = \cos\psi' \cos\omega t. \qquad l_2 = \cos\psi$$
$$m_1 = \cos\psi' \sin\omega t. \qquad m_2 = 0$$
$$n_1 = \sin\psi' \qquad n_2 = \sin\psi$$

Now the angle of incidence of radiation on the silo roof

$$= LOS - \psi$$
$$\cos\phi = l_1 l_2 + m_1 m_2 + n_1 n_2$$
$$= \cos\psi' \cos\psi \cos\omega t + \sin\psi' \sin\psi$$
$$= 0{\cdot}57 \cos\omega t + 0{\cdot}31$$

The south facing wall of the silo is parallel to the earth's surface in latitude $(\psi - \pi/2)$.

Hence the direction cosines are

$$l_3 = \sin\psi$$
$$m_3 = 0$$
$$n_3 = -\cos\psi$$

If θ = angle of incidence on the wall :

$$\cos\theta = \cos\psi' \sin\psi \cos\omega t - \sin\psi' \cos\psi$$
$$= 0{\cdot}72 \cos\omega t - 0{\cdot}25$$

APPENDIX III

Propagation of Temperature Waves into Packed Raw Sugar

Consider a semi-infinite mass of packed raw sugar on one side of a plane boundary. At any instant the temperature of the boundary is uniform. The temperature varies with time according to :

$$T = T_0 \cos\omega t \qquad (1)$$

Heat flow in the sugar is perpendicular to the boundary and obeys the equation :

$$\frac{\partial^2 T}{\partial x^2} = \frac{1}{\alpha}\frac{\partial T}{\partial t} \qquad (2)$$

The solution of equation (2) which satisfies the boundary condition (1) is :

$$T = T_0 \cos\left\{\omega t - \frac{x}{\sqrt{(2\alpha/\omega)}}\right\} e^{-x\sqrt{(\omega/2\alpha)}} \quad (3)$$

This equation represents a wave of wavelength $\lambda = 2\pi\sqrt{\frac{2\alpha}{\omega}}$, with an attenuation coefficient $\beta = \sqrt{\frac{\omega}{2\alpha}}$

The relevant constants for raw sugar are :

$\rho = 910$ kg/metre^3
$c = 1{,}250$ joules/kg
$k = 0{\cdot}161$ watts/metre °C.

Hence $\alpha = \frac{k}{\rho c} = 1{\cdot}42 \times 10^{-7}$ metres^2/sec.

Daily Temperature Variation

$$\omega = \frac{2\pi}{24} \text{ hours}^{-1} = 7{\cdot}26 \times 10^{-5} \text{ sec}^{-1}$$

So that $\lambda = 2\pi\sqrt{\frac{2 \times 1{\cdot}42 \times 10^{-7}}{7{\cdot}2 \times 10^{-5}}}$
$= 0{\cdot}40$ metres

$$\beta = \sqrt{\frac{7{\cdot}2 \times 10^{-5}}{2{\cdot}84 \times 10^{-7}}}$$
$= 16$ metres^{-1}

Seasonal Temperature Variations :

$$\omega = \frac{2\pi}{8766} \text{ hours}^{-1} = 1{\cdot}99 \times 10^{-7} \text{ sec}^{-1}$$

So that $\lambda = 7{\cdot}5$ metres

$\beta = 0{\cdot}83$ metres^{-1}

The values of β are such that the amplitude of the daily temperature wave decreases to 10% of its boundary value after a penetration of 14 cm ; that of the seasonal wave after a penetration of 2·8 metres.

These figures, together with the wavelengths, were confirmed by the analogue measurements.

Acknowledgements

Acknowledgment is made to E. T. Moss for information regarding the thermal properties of the materials considered, to H. C. S. de Whalley, Director of Research, and to the Directors of Tate & Lyle Ltd. for permission to publish this paper.

Notation

T = temperature
x, y, z = rectangular coordinates
ρ = density
c = specific heat
k = thermal conductivity
t = time
$\nabla^2 = \frac{\partial^2}{\partial x_2} + \frac{\partial^2}{\partial y^2} + \frac{\partial^2}{\partial z^2}$
α = thermal diffusivity
V = electric potential
R = resistance
C = capacitance
τ = time constant
N_R = intensity of radiation on the roof
N_W = intensity of radiation on the south wall
N_0 = solar constant
= 980 watts/metre^2 in London allowing for atmospheric absorption
R_l = thermal resistance
C_l = thermal capacity
m = mass per unit area of a layer
d = thickness of a layer
W = % moisture
$\omega = 2\pi \times$ frequency
λ = wavelength
β = attenuation coefficient
ψ = latitude = 51½° for London
ψ' = latitude of the tropics = 23½°
l, m, n = direction cosines
ϕ = angle of incidence on the roof
θ = angle of incidence on the south wall

References

[1] Anon.; *Mechanical Handling* 1954 **41** 115.
[2] Paschkis, V. and Baker, H. D.; *Trans Amer Soc. Mech. Engrs* 1942 **64** 105.
[3] Jakob, M.; Heat Transfer, Chapman & Hall, London, 1949, Vol. **1**, Ch. 20.
[4] Lawson, D. I. and McGuire, J. H.; *Engineer* 1953 **196** 217 and 249.

Chemical Engineering Science, 1955, Vol. 4, pp. 111 to 118. Pergamon Press Ltd.

Longitudinal diffusion in liquid flow through an annulus between a stationary outer cylinder and a rotating inner cylinder

P. Croockewit, C. C. Honig and H. Kramers
Laboratorium voor Physische Technologie, Technische Hogeschool, Delft, Netherlands

(*Received* 12 *February* 1955)

Summary—The longitudinal mixing produced in a liquid which flows through the space between a stationary outer cylinder and a rotating cylindrical core can be interpreted as the result of an apparent longitudinal diffusivity. For various dimensions and rotor speeds the value of the diffusion coefficient has been measured by means of the frequency response analysis.

Résumé—Dans un liquide, qui se trouve dans l'espace annulaire entre deux parois cylindriques, une rotation du cylindre intérieur produit un mélange en direction axiale. Ce phénomène peut être interprété comme le résultat d'un coefficient apparent de diffusion longitudinale. La valeur de ce coefficient a été determiné dans des conditions diverses au moyen de l'analyse de réponse en fonction de la fréquence.

Introduction

In a previous article [1] attention has been drawn to the use of frequency response analysis as a means of determining the distribution of residence times. This analysis consists of introducing a sinusoidally varying signal in the flow at the inlet of the flow system and of measuring the amplitude ratio and the phase shift between the signals at two or more places along the main flow path at various frequencies.

The result of such an analysis can be compared with the calculated behaviour of relatively simple models such as a "perfect" mixer, a cascade of perfect mixers, or "perfect" piston flow. The latter shows no damping of the signal but only a phase shift caused by the distance-velocity lag. This kind of flow is approached in the turbulent flow of a fluid through a straight length of pipe and through packed beds, but a still significant deviation may occur as a consequence of mixing in the direction of flow. If this mixing is of a sufficiently random nature, it can be accounted for mathematically by assigning an apparent coefficient of diffusion, or a longitudinal diffusivity, to the fluid stream. Thus, if longitudinal diffusion occurs in a flow system, the diffusivity can be determined by carrying out a frequency response analysis.

The present paper reports on such measurements for the flow of a liquid through the annular space between a rotating inner cylinder and a concentric stationary outer cylinder. This particular choice was mainly determined by the fact that the flow condition in such a "reactor" depends primarily on the geometry of the system and on the rotational speed of the inner cylinder. Taylor [2] has discovered that above a critical speed a regular pattern of toroidal vortices is set up which have about the same height as the distance between the inner and the outer cylinder. At much higher speeds the vortices become irregular, and a more random turbulence is obtained. Fage [3] has shown that the axial flow velocity has only a secondary influence on these phenomena. In view of this available information, it could be hoped that an interpretation of measured diffusivities would be possible.

Furthermore, the system chosen is of some interest for practical application mainly because a fairly uniform degree of agitation can be adjusted independently of the main flow rate. This special feature has been used, for instance, for liquid-liquid contacting such as extraction [4] and heterogeneous liquid reactions. An example of a reaction in this kind of equipment has been given by Revallier [5] for the continuous

nitration of mono-chloro-mono-nitrobenzene with mixed acid. Parikh [6] has reported measurements on the heat transfer between the flow of water and oil and the outer cylindrical wall in a similar apparatus. For such applications it is desirable to know whether or not the longitudinal mixing impairs the effect of the continuous operation.

Calculations

Suppose we have a reactor through which a liquid flows with uniform velocity $\bar{u}$ (Fig. 1). The flow is such that a constant diffusion coefficient, D, exists in longitudinal direction. If we have the liquid flowing in with a variable concentration, C, the following differential equation obtains :

$$D\frac{\partial^2 C}{\partial y^2} - \bar{u}\frac{\partial C}{\partial y} - \frac{\partial C}{\partial t} = 0. \qquad (1)$$

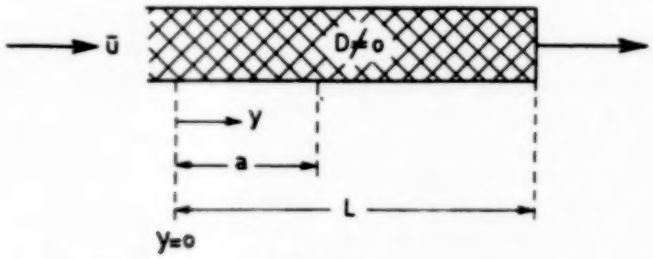

Fig. 1. One-dimensional flow with longitudinal diffusion.

Here, C can also be considered to be the deviation from the average value of the concentration. If C varies sinusoidally, we may substitute :

$$C = X e^{i\omega t}. \qquad (2)$$

thus representing C by a vector X rotating in the complex plane with an angular frequency ω. With (2) equation (1) becomes an ordinary linear differential equation :

$$D\frac{d^2X}{dy^2} - \bar{u}\frac{dX}{dy} - i\,\omega\,X = 0. \qquad (3)$$

In order to determine D, the amplitude ratio, α, of C between $y = a$ and $y = 0$ is measured, together with the phase shift, ϕ, between the two signals, at various frequencies. The values of the vector X at $y = a$, and $y = 0$ are related to each other via α and ϕ in the following manner :

$$\frac{X_a}{X_0} = \alpha\, e^{-i\phi}. \qquad (4)$$

Thus, in order to compare α and ϕ with the theory, the complex transfer function X_a/X_0 has to be calculated from (3).

The appropriate boundary conditions are :

$$\left.\begin{aligned} y = 0 \quad & X = X_0 \\ y = L \quad & \frac{\partial X}{\partial y} = 0 \end{aligned}\right\} \qquad (5)$$

The latter condition has been discussed by Danckwerts [7] and also in [1]. The solution of (3) and (5) is

$$\frac{X_a}{X_0} = e^{p_2 a}\,\frac{1 - \frac{p_2}{p_1}\,e^{(p_1 - p_2)(L-a)}}{1 - \frac{p_2}{p_1}\,e^{(p_1 - p_2)L}}, \qquad (6)$$

with

$$\frac{p_1}{p_2} = \frac{\bar{u}}{2D}\left(1 \pm \sqrt{1 + 4\,\frac{i\omega D}{\bar{u}^2}}\right). \qquad (7)$$

It is easily shown that :

$$\operatorname*{Lim}_{D\to 0}\frac{X_a}{X_0} = e^{-i\omega\frac{a}{\bar{u}}}, \quad \text{or } \alpha = 1 \text{ and } \phi = -\omega\frac{a}{\bar{u}},$$

which represents a pure distance-velocity lag. Also :

$$\operatorname*{Lim}_{D\to\infty}\frac{X_a}{X_0} = 1, \text{ or } \alpha = 1 \text{ and } \phi = 0,$$

which means that in a perfect mixer the concentration has the same value at every point.

The general result (6) is somewhat complicated, but under certain conditions it can be simplified to :

$$\frac{X_a}{X_0} = e^{p_1 a}. \tag{8}$$

In the present work we chose $a \cong \frac{1}{2}L$, whereas $\bar{u}L/2D$ was of the order of unity. In that case it can be shown that (8) is a sufficiently accurate approximation of (7) if the measuring frequency, ω, is chosen to be greater than $3\bar{u}^2/D$.

It is to be noted that eq. (8) is the solution of (3) if the second boundary condition in (5) is replaced by

$$y = \infty, \quad X = 0.$$

Thus the finite length of the reactor introduces an end effect which can be circumvented by taking a sufficiently small with respect to L and by measuring at relatively high frequencies.

The amplitude ratio, α, and the phase shift can be calculated from eq. (8) to be :

$$\left.\begin{aligned} \alpha &= \\ &\exp\left[-N_D\left\{\frac{1}{\sqrt{2}}\left(\sqrt{1+\frac{4\omega^2\tau^2}{N_D^2}}+1\right)^{1/2}-1\right\}\right] \\ \phi &= -N_D\frac{1}{\sqrt{2}}\left(\sqrt{1+\frac{4\omega^2\tau^2}{N_D^2}}-1\right)^{1/2} \end{aligned}\right\} \tag{9}$$

where

$$N_D = \frac{\bar{u}a}{2D} \quad \text{and} \quad \tau = \frac{a}{\bar{u}}. \tag{10}$$

Fig. 2 gives as an example the dependency of α and ϕ on N_D for several values of $\omega\tau$. An experiment under a given set of conditions gives, for a chosen value of $\omega\tau$, a result for α and ϕ.

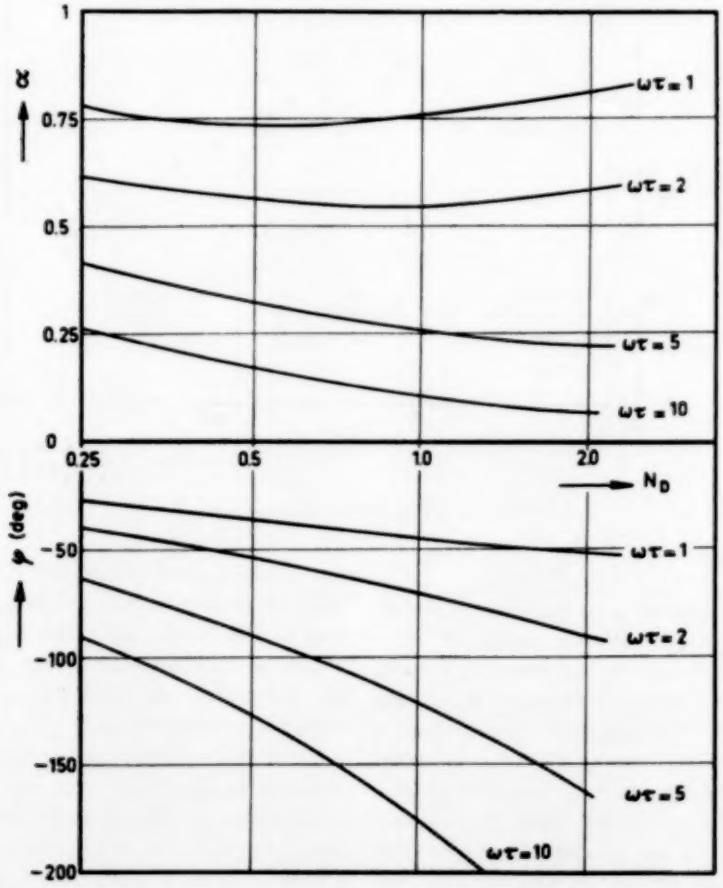

FIG. 2. Calculated relations between α and N_D and between ϕ and N_D for different values of $\omega\tau$.

From either of these a value of N_D can be found, $(N_D)_a$ and $(N_D)_\phi$ respectively. If $(N_D)_a$ and $(N_D)_\phi$ agree with each other, and if the same values of these quantities are found at other measuring frequencies, it may be concluded that the longitudinal mixing can be described as a diffusion process. From the lines in Fig. 2 it can be seen that generally the phase shift will yield more dependable values of N_D than the amplitude ratio. This is especially true for relatively low frequencies where the curve for α shows a weak minimum.

Water was fed to the reactor at constant flow rate and measured with a rotameter. With this main flow a relatively small pulsating stream of a concentrated NH_4Cl-solution was mixed, so that a practically constant feed rate to the reactor was obtained with a sinusoidally varying salt concentration. The pulsating flow of the concentrated salt solution was obtained by displacing the solution with oil, the flow of which was modulated by a combination of a small constant rate feed pump and a buffer volume closed at one end with a reciprocating piston. The frequency

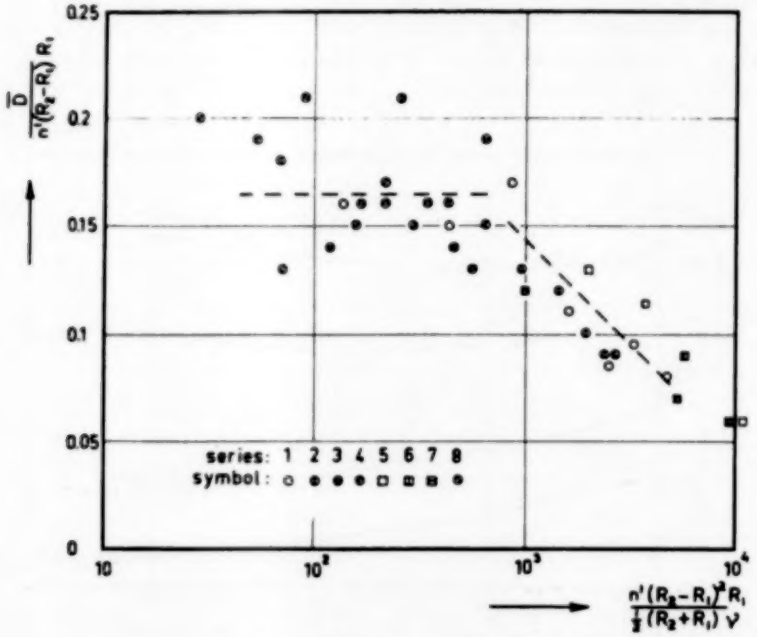

FIG. 3. Experimental arrangement.

EXPERIMENTAL PART

The experimental arrangement is shown in Fig. 3. The "reactor" (height 38 cm) consisted of a stationary outer cylinder of "perspex." Two of these were available with inner radii of $R_2 = 4{\cdot}52$ and 6·35 cm. The rotating solid cylinder had a steel core; the outer diameter, $2R_1$, was adjusted to different values by covering the core with a layer of modelling wax after which it was machined on a lathe to the wanted diameter. The rotational speed of the rotor was adjusted by means of a variable speed drive.

and the amplitude of the piston could be adjusted. The salt concentration at the inlet of the reactor was purely sinusoidal. The same applies to the electrical conductivity of the solution which at the concentrations used (up to 1·5 g/l) is linear with the concentration.

Near the inlet and about half way the reactor a small conductivity cell was attached to the outer cylinder. The distance between the cells, a, was 16·3 cm. The conductivity of the liquid in either cell could be recorded. By comparing the records of both cells under a given set of conditions

Table 1. *Summary of results for water at room temperature. Measuring distance, a, between the cells* 16·3 *cm.*

Series	R_2 (*m*)	$R_2 - R_1$ (*m*)	n (*rev/min*)	$D\phi$ $\left(10^{-4}\frac{m^2}{sec}\right)$	D_a $\left(10^{-4}\frac{m^2}{sec}\right)$	$\overline{D}$ $\left(10^{-4}\frac{m^2}{sec}\right)$	$\frac{\overline{D}}{n'(R_2-R_1)R_1}$	$\frac{n'(R_2-R_1)^2R_1}{\frac{1}{2}(R_2+R_1)\nu}$
1	0·0452	0·0249	22	0·3	–	0·3	0·16	140
			70	0·85	1·0	0·9	0·15	440
			135	2·1	1·7	1·9	0·17	870
			250	2·3	2·6	2·4	0·11	1610
			390	2·6	3·1	2·8	0·085	2500
			520	3·1	5·2	4·1	0·095	3300
			735	4·2	5·3	4·8	0·08	4700
2	0·0452	0·0157	22	0·3	0·3	0·3	0·18	70
			70	1·0	1·5	1·2	0·21	230
			135	1·6	1·7	1·7	0·16	440
			200	2·1	2·3	2·2	0·15	650
			300	2·9	2·9	2·9	0·13	970
			450	4·1	4·1	4·1	0·12	1460
			600	4·2	5·7	5·0	0·10	1950
			735	4·8	5·7	5·2	0·09	2380
3	0·0452	0·0077	135	1·1	0·5	0·9	0·14	120
			250	1·9	1·8	1·9	0·16	220
			390	3·1	2·8	3·0	0·16	350
			520	3·4	2·8	3·2	0·14	460
			640	4·0	–	4·0	0·13	570
			735	6·9	7·9	7·1	0·19	660
4	0·0452	0·0051	22	0·19	0·18	0·19	0·25	9
			70	0·4	0·4	0·4	0·20	29
			135	0·9	0·9	0·9	0·19	55
			250	1·3	1·0	1·2	0·13	71
			390	2·4	1·5	2·1	0·15	160
			520	3·1	3·1	3·1	0·17	210
			735	3·8	3·8	3·8	0·15	300
5	0·0635	0·0432	135	2·5	2·5	2·5	0·13	2000
			250	4·0	3·6	3·9	0·11	3700
			735	5·1	6·7	6·0	0·06	10900
6	0·0635	0·0340	450	7·6	6·3	7	0·09	5600
			735	7·8	12	9	0·06	9100
7	0·0635	0·0234	135	2·6	2·6	2·6	0·12	980
			735	7·0	10	8	0·07	5200
8	0·0452	0·0157	135	2·3	2·0	2·2	0·21	92•
			250	2·3	4·0	3·0	0·16	169•
			450	3·2	–	3·2	0·09	2660†

• $\nu = 4{\cdot}8 \times 10^{-6}\ m^2/sec$ † $\nu = 0{\cdot}55 \times 10^{-6}\ m^2/sec$

the amplitude ratio α and the phase shift ϕ between the two signals were measured. Although the conductivity measurement in itself had a precision of about 1%, the error in α, as derived from the

recordings, is estimated to be 5% or even greater for high damping ratios. The accuracy of ϕ was somewhat better but it decreased with higher measuring frequencies. The error in $\omega\tau$ was not greater than 1%.

An experimental run under a given condition consisted of the determination of α and ϕ for 3 or 4 values of $\omega\tau$ chosen between 1 and 10. By then comparing the values found for α and ϕ with the calculated graphs of α and ϕ vs. $\omega\tau$, for different values of N_D an estimate was obtained for the values of $(N_D)_\alpha$ and $(N_D)_\phi$ respectively. As can be seen from Fig. 2 a variation in ϕ of, say, 1% may cause a variation in $(N_D)_\phi$ between 3 and 10% depending on the value of $\omega\tau$ used. The determination of $(N_D)_\alpha$ from α values is still more uncertain. Consequently, the possible error in D_ϕ may sometimes be about 15% and in D_α even as high as 30%.

In Table 1 all results of these experiments have been assembled. The D_ϕ and D_α values have been given separately. Except for a few cases the agreement between D_ϕ and D_α is fair, considering the uncertainties involved. This in general justifies the description of the longitudinal mixing by means of an effective diffusivity. For further calculations an average value $\overline{D}$, between D_ϕ and D_α has been used with preference towards the value of D_ϕ.

The linear velocity of the upward flow of the liquid varied in these runs between 0·002 and 0·007 m/sec, which is small compared with the circumferential rotor speeds used (0·05-6 m/sec), and it could be expected that in these cases $\overline{D}$ would not depend on $\bar{u}$. In 10 separate experiments under widely different conditions where besides the frequency also the main flow velocity was varied, no significant influence of $\bar{u}$ on $\overline{D}$ could be detected.

Discussion

All measurements were taken at a higher rotational speed than the critical value at which the vortex pattern appears. For this critical speed, $n_c = 60\, n_c'$, Taylor's formula [2] gives as a first approximation :

$$\frac{n_c'\,(R_2 - R_1)\,R_1}{\nu}\left(2\,\frac{R_2 - R_1}{R_2 + R_1}\right)^{1/2} = 6{\cdot}5. \qquad (11)$$

For the present experiments the calculated n_c varied between 0·5 and 6 rev/min, whereas the lowest value of n used was 22 rev/min.

From visual observation with water to which some aluminium powder had been added it was ascertained that the height of the vortices was somewhat greater than the width of the annulus $(R_2 - R_1)$ and increased only slightly with increasing rotational speed. Such a change in height of the vortices was discontinuous, since the reactor can only contain an even number of them. At the same time it was found that the direction of the striae to be observed near the outer wall did not change much with the speed of the rotor. This indicates that, in first approximation, the circumferential speeds of the rotor and of the vortices are proportional to each other.

In order to relate the apparent diffusivity to the flow conditions this transport coefficient has to be compared to the product of a characteristic length and a significant velocity, for which then should be taken the height of the vortices and their speed of rotation respectively. Instead of these quantities the product of $(R_2 - R_1)$ and of $n'R_1$ was chosen to form the dimensionless ratio : $\overline{D}/n'R_1\,(R_2 - R_1)$. As can be seen from Table 1 and from Fig. 4 this ratio is approximately constant over the lower range of rotor speeds used. In this range 70% of the values of $\overline{D}/n'R_1\,(R_2 - R_1)$ lie between 0·14 and 0·19. The large deviations must be attributed to random errors, since no systematic trend could be detected.

Two runs in which the viscosity was increased 5-fold by using a glycerol-water mixture (Table 1, series 8) show no appreciable deviation from the other results. This indicates that the transport is entirely convective and that the molecular diffusivity of the salt molecules in the liquid has no influence once the toroidal flow pattern exists. The reported values of $\overline{D}$ are higher than the molecular diffusivity by a factor of about 10^5.

When the rotor speed is increased a transition can be observed from the regular vortex pattern to a more general turbulence. For a few cases the rotational speed, n_t, at which this gradual transition occurred was estimated visually. It can be seen from Table 2 that the dimensionless

VOL. 4 1955

group in TAYLOR's criterion, eq. (11), has no significance here and that the width of the annulus apparently has a relatively stronger influence on the onset of general turbulence.

Table 2. Rotor speed, n_t, at which general turbulence sets in; water, room temperature.

R_2, m	0·0452	0·0452	0·0452
$R_2 - R_1$, m	0·0249	0·0157	0·0077
n_t, rev/min	150	300	> 900
$\frac{n_t'(R_2-R_1)R_1}{\nu}\left(2\frac{R_2-R_1}{R_2+R_1}\right)^{1/2}$	1100	1500	> 1900
$\frac{n_t'(R_2-R_1)R_1}{\nu}\left(2\frac{R_2-R_1}{R_2+R_1}\right)$	970	970	> 820

Table 2 suggests the following criterion for general turbulence to appear between a rotating inner cylinder and a stationary outer cylinder:

$$\frac{2\,n_t'\,(R_2 - R_1)^2\,R_1}{\nu\,(R_2 + R_1)} \cong 1{,}000. \qquad (12)$$

In Fig. 4 the dimensionless diffusion number has been plotted against $2\,n'\,(R_2 - R_1)^2 R_1/\nu\,(R_2 - R_1)$. It is evident that the value of $\overline{D}/n'(R_2 - R_1)R_1$ significantly decreases as the criterion of eq. (12) is passed. This is in accordance with the visual observations and the relative lowering of $\overline{D}$ may be mainly attributed to the decrease of the scale of turbulence in this region as the rotor speed is increased.

The above conclusions are far from being exact, but they may provide a basis for estimating the importance of the back-mixing effect if a physical operation or a chemical reaction is carried out in this kind of apparatus. Apart from the characteristics of the process involved, the value of $\bar{u}L/2D$ (L = length of reactor) indicates whether the influence of longitudinal diffusion need to be considered. If $\bar{u}L/2D > 1$, e.g. 10 or more, the influence of back-mixing on the result of the

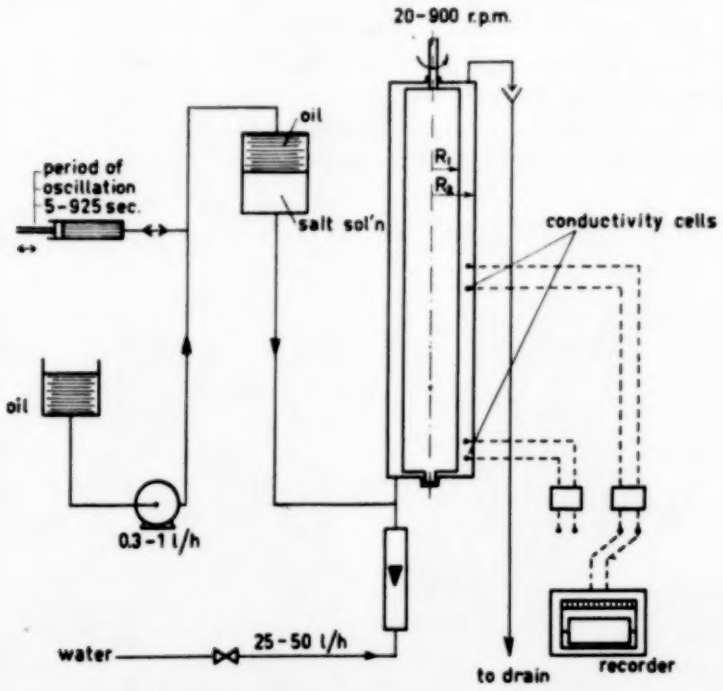

FIG. 4. Proposed general correlation between the apparent diffusivity $\overline{D}$, the dimensions of the annulus and the rotational speed of the inner cylinder.

process will generally be negligible. This applies to all of PARIKH's heat transfer measurements [6]. If on the other hand, for instance, with slow chemical reactions and long residence times, $\bar{u}L/2D \ll 1$ then the reactor behaves like a perfect mixer. In such a case back-mixing can be suppressed to some extent by mounting horizontal rings either on the rotor or on the stator which just leave sufficient clearance for the main liquid stream to pass but which prevent back-mixing between the different compartments.

ACKNOWLEDGEMENT

The authors gratefully acknowledge the cooperation of P. J. KREYGER who took part in the measurements.

NOTATION

a = distance between points of measurement (m)
C = concentration
D = coefficient of diffusion, used in theory (m^2/sec)
$\overline{D}$ = average apparent diffusivity, from measurements (m^2/sec)
$i = \sqrt{-1}$
L = length of the flow system, taken from $y = 0$ (m)
n' = speed of rotation of the rotor (rev/sec); $n = 60n'$ (rev/min)
$N_D = \bar{u}a/2D$
R_1 = outer radius of inner cylinder (m)
R_2 = inner radius of outer cylinder (m)
t = time (sec)
$\bar{u}$ = average liquid velocity in direction of flow (m/sec)
X = complex concentration deviation vector
y = coordinate in direction of flow (m)
α = amplitude ratio of signal between two measuring points
ν = kinematic viscosity (m^2/sec)
τ = average residence time = $a/\bar{u}$ (sec)
ϕ = phase shift of signal between two measuring points (radians)
ω = circular frequency (radians/sec)

VOL. 4 1955

REFERENCES

[1] KRAMERS, H. and ALBERDA, G.; *Chem. Eng. Sci.* 1953 **2** 173.
[2] TAYLOR, G. I.; *Proc. Roy. Soc.* A 1935 **151** 494, 1936 **157** 546 and 565.
[3] FAGE, A.; *Proc. Roy. Soc.* A 1938 **165** 501.
[4] SHORT, J. F. and TWIGG, G. H.; *Ind. Eng. Chem.* 1951 **43** 2032.
[5] REVALLIER, L. J.; Thesis, Delft 1952.
[6] PARIKH, C. K.; Thesis, Imperial College, London 1952.
[7] DANCKWERTS, P. V.; *Chem. Eng. Sci.* 1953 **2** 1.

Chemical Engineering Science, 1955, Vol. 4, pp. 119 to 129. Pergamon Press Ltd.

Flow of granular material through a circular orifice

F. C. Franklin and L. N. Johanson
Chemical Engineering Department, University of Washington

(*Received* 25 *February* 1955)

Summary—Data have been obtained for the flow of granular materials through horizontal circular orifices, and correlated in the form of an empirical equation and nomograph with a mean deviation of ± 7%. Data for inclined circular orifices are also represented by the same expression, when modified by a term involving the angle of inclination of the orifice as the only additional variable. The variables of importance influencing mass flow rate are the orifice diameter, particle diameter, particle density, and the angle of repose of the material, provided bed height and column-to-orifice diameter ratio exceed certain minimum values.

Particle size ranged from 0·03 to 0·2 inches, particle density from 7·3 to 676 lb./ft.^{3}, and orifice diameter from 0·236 to 2·28 inches.

Previous results for the flow of granular materials through restrictions are reviewed, and are found to be in reasonable agreement with the present correlation.

Résumé—Les auteurs étudient l'ecoulement de matériaux granulaires au travers d'orifices circulaires et met les résultats sous la forme d'une équation empirique et d'un abaque avec une précision de ± 7%. Pour des orifices circulaires inclinés, la même expression reste valable en tenant compte de cette inclinaison par une seule variable additionnelle. Pourvu que le lit ait une certaine épaisseur et que le rapport du diamètre de la colonne à celui de l'orifice dépasse certaines valeurs minimum, les variables qui ont une influence importante sur la vitesse d'écoulement sont le diamètre de l'orifice, le diamètre et la densité des particules, l'angle de repos du matériau.

Ces variables sont limitées aux valeurs suivantes :

– dimension des particules	0,03 à 0,02 inch	(0,076 à 0,0508 cm)
– densité des particules	7,3 à 6,76 lb/ft^3	(0,117 à 0,107 g/cm^3)
– diamètre de l'orifice	0,236 à 2,28 inch	(0,6 à 5,8 cm)

Les auteurs trouvent des résultats en accord avec les données antérieures.

The need for quantitative information on the variables determining the rate of flow through a restriction has grown with the advent of large-scale processes employing moving beds of granular catalyst or other solid. Knowledge of fluid flow principles is of little help in such problems, since granular material systems, either static or moving, deviate markedly from such principles. This is due mainly to the bridging of solid resulting from the forces exerted by a particle on neighbouring wall or particles.

Previous investigations of granular solids flow have been reported. The least generalized of these was that of Newton, Dunham, and Simpson [1] on the flowrate of 0·1 to 0·2 inch cylindrical clay cracking catalyst particles through a horizontal orifice of a flat bottomed container. The angle of repose of the material was reported as 38° and the minimum orifice diameter about six times the particle diameter. The empirical equation proposed relates mass flow rate, W, to orifice diameter, D_o, and bed height, H, as follows :

$$W = 8{\cdot}50\, D_o^{2{\cdot}96}\, H^{0{\cdot}04} \qquad (1)$$

Since this equation is specific, it gives no information about the effect of particle diameter, angle of repose, or other possible fundamental variables.

Deming and Mehring [2] studied the flowrate of a variety of materials through an inverted truncated cone orifice. Flow rate was found to vary with a power of the orifice size, and to be influenced by the size and apparent density of the particles, the angle of repose of the materials,

and the cone angle. The equation obtained would not be expected to apply to an orifice through a plate, that is, a cone angle of 180°. The equation was of the form :

$$t = \frac{\mu_1}{D_o^{2.5} D_p} \left[0.201 + (39.2 + 2.58 \sin \tfrac{1}{2}\phi) \left(\frac{D_p}{D_o} + 0.130 - 0.161\, \mu_1 \right) \right] \qquad (2)$$

which relates time of flow, t, to the tangent of the static angle of repose, μ_1, orifice diameter, D_0, particle diameter, D_p, and the cone angle, ϕ.

The most generalized investigation was reported by Takahasi [3] who studied many types of sand, shot, vegetable seeds, and mixtures of sand and sulphur and sand and talcum. His result was expressed by the empirical equation :

$$t = \sqrt{\frac{b}{g}}\, D_o^{2.5} \left[f(\mu_2) + a \left(\frac{D_p}{D_o} \right) \right] \qquad (3)$$

Where a and b are constants dependent only on the system of units used : g is gravitational acceleration, $f(\mu_2)$ is a power function of the tangent of the surface kinetic angle of repose, and other terms are as previously defined.

The appearance of the D_o in two terms tends to produce a curved line on a log-log plot of flow rate vs. D_o. Some examples of the observed data given appear to have some curvature in such a plot, but most could equally well be expressed as a straight line, especially when one considers the size of the apparatus used and the resulting probable accuracy. It is also quite likely that the data on large particles were excessively influenced by the container walls, which Takahasi did not consider. In addition there is some uncertainty whether reciprocal volume flow rate is to be based upon bulk volume or particle volume.

In view of this meagre and uncertain information, the present investigation was begun to study the effect of the following variables : (1) orifice diameter, (2) particle diameter, (3) particle density, (4) angle of repose, both static and kinetic, (5) bed height, (6) void fraction, and (7) angle of inclination of the orifice. Preliminary study had indicated flow rate could also be influenced by the following factors : (1) particle to orifice ratio exceeding 0·2, (2) orifice to column diameter ratio exceeding 0·16, and (3) bed height less than one column diameter. Correlation was therefore restricted to values within these limits. In addition, particles selected were of sufficient size and weight that effects of electrostatic attraction or repulsion were negligible. All particles were air dried to avoid agglomeration.

Experimental

Material was poured loosely into vertical glass columns and allowed to flow downward through a circular orifice in a $\frac{1}{16}$ inch plate. The orifice was horizontal and centered at the column bottom except for the runs investigating the effect of angle of inclination from the horizontal. Flow rate was obtained by determining the weight of material flowing in a given time interval, measured by spotwatch. This method allowed several rate values to be obtained during a run as a test of rate variation with decreasing bed height. Column diameter ranged from 1·76 to 8·81 inches depending upon the diameter of the orifice used. Four smaller columns were used to study the wall effect at constant orifice diameter. The inner surfaces of the columns were roughened with drafting tape to study the effect of wall roughness.

Particle diameter ranged from 0·03 to 0·2 inches. The diameter was determined by the average of direct measurement for large particles, and by arithmetic average screen mesh size of the fraction for smaller particles.

Particle density was measured by the immersion method, the fluid used depending on the porosity of the particle. It was felt that actual particle density, including internal pores was a more fundamental variable than either bulk or true material density. Bulk density and the related void fraction were found to be dependent on the manner of placing the material in the column, whereas the flowrate, once started, is not so dependent. It has been found also that the void fraction of the static bed is not necessarily the same as for the moving bed. On the other hand, true material density could not be correlated with flowrate variation. This appears to indicate

VOL. 4 1955

that the flowrate is a volumetric, particle-spatial phenomenon.

For porous materials mercury was used as the immersion fluid, with a vacuum being utilized to remove air from the inter-particle voids in order to reduce the possibility of unfilled voids. For the non-porous particles water was used. A thin wax coat of negligible volume was applied to the puffed rice making possible the use of water as immersion fluid since mercury would have both penetrated and compressed the particles. The particle density was varied from 676 lb. per cu. ft. for lead shot to 7·34 lb. per cu. ft. for puffed rice.

Static bed void fractions were calculated from particle density and bulk density values for the static bed.

The angle of repose would appear to be an important characterization factor for less easily defined particle properties, such as shape, roughness, effective size and effective void fraction. Previous workers have used the static angle of repose [2], and the surface kinetic angle of repose [3]. The first may be defined as the maximum angular deviation from horizontal of the surface of a static pile of granular material Its tangent is defined here as μ_1. The second is the slope of a continuously moving surface of a pile of granular material (tangent $= \mu_2$). Observation of the "shear angle" between relatively fast moving and slow moving particles as granular material cones toward an orifice suggests that such an internal angle may be more proper fundamentally. Though this angle was not measureable with any precision in the columns used, an internal angle believed similar (tangent $= \mu_3$) was easily and reproducibly measured in an apparatus [4] constructed for this purpose. This apparatus was also used for determining static and surface kinetic angles of repose.

The apparatus consisted of a rotating drum one foot in diameter and eight inches long, with axis fixed in a horizontal position, and having a front face of transparent lucite plastic through which the various angles of repose could be observed. The curved surface was roughened to prevent slippage of the material along this wall. The drum could be rotated at constant speeds, from very low rates to about five or six r.p.m. The maximum angle of repose attainable by the solid before moving or cascading downward was recorded as the static angle of repose. Kinetic angles were measured with the particles rolling downward over the slanting surface at essentially a constant rate. The internal kinetic angle with tangent defined here as μ_3 could be observed as the plane of contact between the downward moving stream and the stream being carried upward by the motion of the rotating drum as shown in Fig. 1. The use of internal kinetic

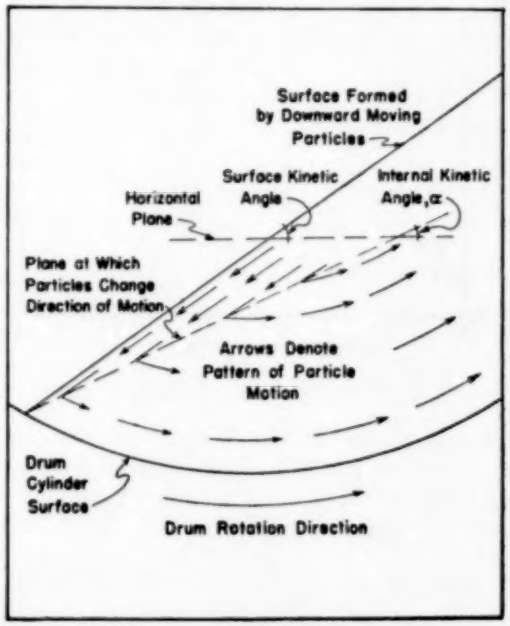

FIG. 1. Surface kinetic and internal kinetic angles of repose.

angle of repose gave a better correlation of the flow rate data than did use of either static or surface kinetic angle. This may have been due in part to the dependence of surface angle upon the rate of rotation of the drum. The effect of the lucite face on the angle of repose appeared negligible, since the surface at the lucite face was not appreciably deformed from that of the bulk of the material in the drum. Intercorrelations of the three angles of repose; static, surface

kinetic, and internal kinetic are shown in Fig. 2. Although this correlation is of adequate precision for this work, it should be accepted with caution in view of the limited knowledge of the factors influencing the various angles of repose.

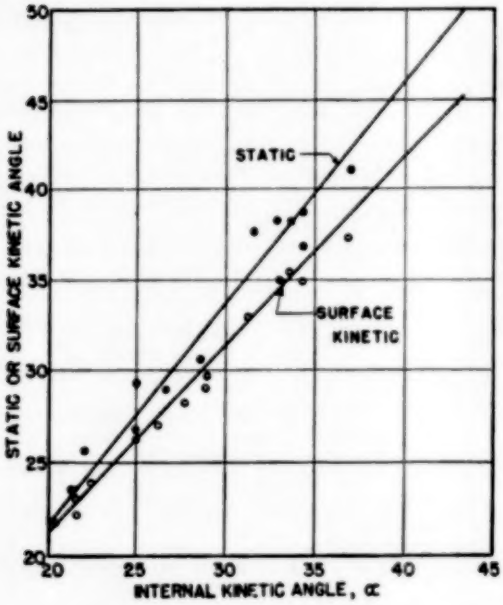

Fig. 2. Inter-relationship of angles of repose.

Results obtained for each of the materials used are summarized in Table I for horizontal orifices, and Table II for inclined orifices. These will be discussed separately.

Horizontal Orifice Results

Preliminary experiments were conducted to determine the influence of the nearness of the column wall upon flow rates. Results obtained varying column size, for an orifice to particle size ratio near the minimum for consistent flow, are shown in Fig. 3. There is an influence on flow rate as orifice and column diameters approach the same value. It is believed that the difference in radii of orifice and column in terms of particle diameters is the pertinent variable. Thus the abcissa expressed as $(D_c - D_o)/D_p$ may be a more general expression of this effect. This term and the one used in Fig. 3 are related; $(D_c - D_o)/D_p = (D_c/D_o - 1)\ D_o/D_p$. When the difference between orifice and column diameter is greater than about 30 particle diameters, the influence of the wall is negligible. In most applications it is relatively easy to obtain this condition, and this was done for all subsequent measurements in this work. This relationship between column and orifice diameter was only slightly influenced by the roughness of the wall.

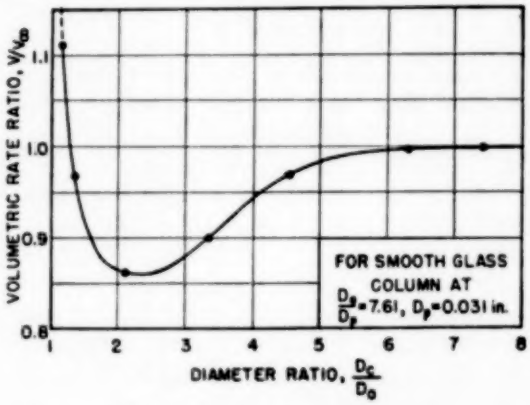

Fig. 3. Influence of container wall upon flowrate.

Straight lines were obtained when the logarithm of the flow rate was plotted versus the logarithm of orifice diameter, so that the influence of the orifice diameter is completely satisfied by one simple factor. This is shown in Fig. 4. The slopes of the lines and hence the exponents of the orifice diameter varied with the material used from about 2·8 to 3·1 with an average value of 2·93. A plot of the exponent versus the static bed void fraction indicated that there was some degree of correlation, the exponent tending to increase with void fraction, but the points were scattered sufficiently that an attempt to express an exact relationship was not believed warranted.

Having determined the influence of the orifice diameter, the remaining influence of other variables would appear in the intercept values at an orifice diameter value of unity in such a log-log plot. Expressing these intercept values of flow rate in units of particle volume rate no further correlation could be found between these values and particle density, void fraction, or bed height, provided that the bed height was

Table I. Horizontal orifice results.

Material	D_o	D_p	ρ_p	ϵ	α	W*	*W (Eq. 5)*
Glass Beads, 16-28 mesh (Scotchlite)	0·236	0·031	173	0·241	25°	0·597	0·484
	0·297					1·06	0·956
	0·422					3·01	2·67
	0·614					8·41	8·00
	1·051					38·52	38·5
Glass Beads, 5 mm borosilicate	1·35	0·196	160	0·359	22·5°	43·0	43·8
	2·28					189·7	202
Ion Exchange Resin spheres, 16-28 mesh	0·236	0·031	92	0·428	21·5°	0·307	0·308
	0·422					1·69	1·70
	0·799					10·27	11·0
Lead Shot, "Dust"	0·236	0·0425	676	0·403	21·5°	1·85	2·12
	0·297					3·83	4·20
	0·422					11·92	11·7
	0·800					72·1	76·0
Lead Shot, No. 12	0·422	0·050	676	0·411	20·2°	11·0	12·0
	0·614					32·1	36·1
	0·800					69·9	78·0
Cracking Catalyst, Used Bead Spheres							
Through 6 mesh	0·799	0·113	80	0·398	28°	4·70	5·08
	0·925					7·48	7·80
	1·051					11·22	11·32
	1·378					27·25	25·2
4-6 mesh	1·378	0·158	80	0·424	26·5°	23·33	22·9
	1·693					39·53	41·8
	1·930					62·3	61·3
Unsized	1·378	0·130	80	0·398	29°	24·03	23·1
	1·930					61·2	61·7
Cracking Catalyst, Clay Cylinders							
New Unsized	1·352	0·185	95	0·508	34°	17·82	19·3
	2·28					82·75	89·0
Used Unsized	1·378	0·130	82	0·442	34·5°	20·70	18·9
	1·93					56·6	50·5
	2·28					81·8	82·5
Puffed Rice	1·35	0·205	7·34	0·373	31·5°	1·65	1·52
	1·93					4·67	4·32
	2·28					8·14	7·05
Crushed Olivine Rock 16-28 mesh	0·236	0·031	207	0·347	33·5°	0·425	0·396
	0·422					2·37	2·19
	0·800					15·81	14·2
4-6 Mesh	1·35	0·158	207	0·335	37°	38·45	41·2
	2·28					181·1	190
Coal (Tono), 16-28 Mesh	0·236	0·031	86	0·530	31°	0·208	0·183
	0·422					1·183	1·01
	0·614					3·35	3·03
	0·800					7·32	6·54

* Each value of W represents the mean of two or more determinations, with an average deviation of less than two per cent.

Table II. Inclined orifice results and comparison with equation 6.

Material	D_o *(in.)*	D_p *(in.)*	*Flow Rate, lb./min. Experimental Results* $\theta = 0°$	$\theta = 30°$	$\theta = 60°$	$\theta = 90°$	*Flow Rate, lb./min. From Equation 6** $\theta = 30°$	$\theta = 60°$	$\theta = 90°$
Glass Beads,	0·50	0·031	4·91	4·47	3·58	2·01	4·57	3·62	2·33
16-28 mesh	0·375		2·39			0·873	2·22	1·76	1·12
" Scotchlite "	0·25		0·717	0·634	0·440	0·254	0·667	0·529	0·340
Lead Shot, " Dust "	0·50	0·0425	21·4	19·9	16·85	11·23	19·9	15·85	10·3
	0·375		8·57	8·04	6·19	3·83	7·96	6·35	4·12
	0·25		2·57	2·21	1·68	1·21	2·39	1·90	1·24

* Based upon data of column 4 for $\theta = 0°$.

greater than the height of the cone formed by the moving particles as they approached the orifice.

No influence of excessive compaction, bridging, or related effects were observed as bed depths were increased, up to the maximum six foot depth studied. This is in agreement with previous work [1, 3], and may indicate that the wall supports the major weight of granular material, eat least in the relatively narrow columns usd in such work.

In a preliminary correlation plot of the reciprocal of the intercept values obtained from Fig. 4 versus particle diameter, it was found that the data could be represented by straight lines if the tangent of the internal kinetic angle of repose μ_s was used as a parameter, in accordance with the following equation;

$$\left(\frac{1}{K} - B\right) \Big/ (D_p - A) = C\,\mu_s + E. \qquad (4)$$

Depending on the values of A and B the family could either be a series of parallel lines or could actually intersect at a finite point. Upon rearrangement the equation may be expressed;

$$\frac{1}{K} = C\,\mu_s\,D_p + E\,D_p - C\,A\,\mu_s - (A\,E - B).$$

or $y = ax_a + bx_b + cx_c + d.$

where $y = 1/K$, $x_a = \mu_s\,D_p$, $x_b = D_p$, $x_c = \mu_s$, $a = C$, $b = E$, $c = -CA$, and $d = -AE + B$. The coefficients a, b, c, and d were evaluated by the method of least squares and incorporated into the basic equation to yield the final empirical result:

$$W = \frac{\rho_p\,D_o^{2.93}}{(6{\cdot}288\,\mu_s + 23{\cdot}16)(D_p + 1{\cdot}889) - 44{\cdot}90} \qquad (5)$$

If eq. (5) is plotted with D_o as abcissa on log-log paper all the data can be represented by a single straight line with a slope of 2·93, the maximum deviation being about $\pm$ 11%, and the mean

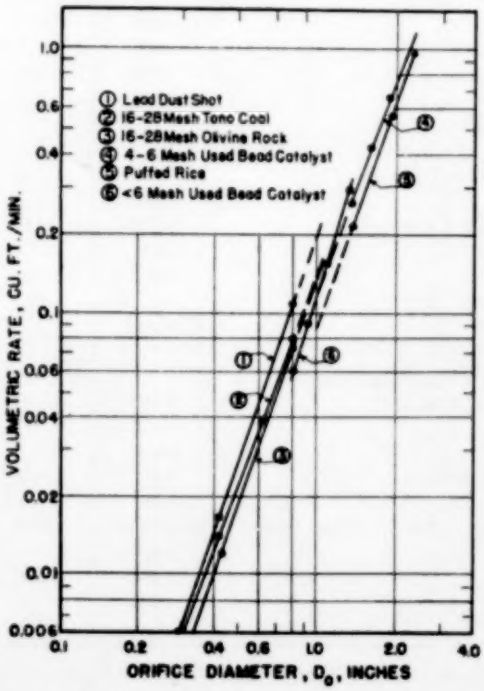

FIG. 4. Influence of orifice diameter upon flowrate.

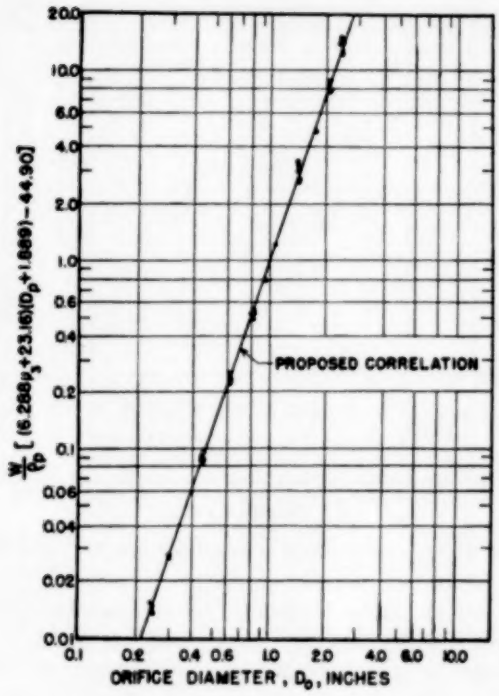

FIG. 5. Proposed flowrate correlation.

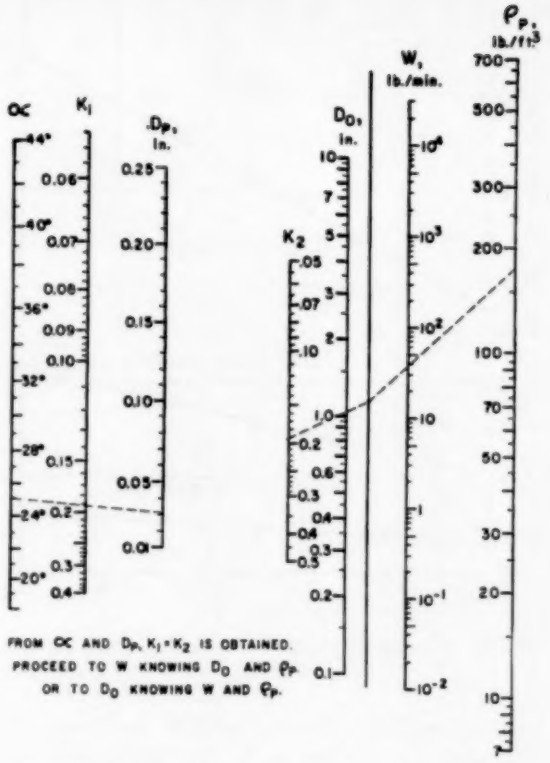

FIG. 6. Nomograph of proposed flowrate correlation, equation (5).

deviation 7%. This correlation is shown in Fig. 5 and Table I. The nomograph, Fig. 6, was constructed on the basis of the above equation to allow more rapid calculation.

INCLINED ORIFICE RESULTS

The effect of the angle of inclination of the orifice, as summarized in Table II, is from the work of GUNDERSON [5]. The lead shot and the glass beads used were the same as used for horizontal orifice studies, and the apparatus and method of determining flow rate were similar. The orifices used were approximately $\frac{1}{4}$, $\frac{3}{8}$ and $\frac{1}{2}$ inch, drilled through $\frac{3}{32}$ inch galvanized sheet metal. The orifice plates were mounted at the truncated end of a two inch diameter cardboard tube, for 30° and 60° inclination. For 90° inclination the orifice was mounted in a side face of a rectangular box of the same diameter as the circular cylinder below which it was attached.

As illustrated by Fig. 7 for lead shot, the data can be represented by straight lines if mass rate of flow is plotted versus the cosine of the angle of inclination from horizontal of the orifice. An extrapolation of such lines to intercept the abcissa at zero flow rate suggests that flow rate will approach zero as the axis of the orifice approaches a line perpendicular to the kinetic angle of repose. Since this is intuitively logical the data were related to the flow rate through a horizontal orifice by means of a multiplying factor involving the angle of inclination of the orifice, and the angle of repose of the granular solid, thus

$$W_\theta = W_0 \frac{\cos \alpha + \cos \theta}{\cos \alpha + 1} \qquad (6)$$

where. W_θ is the flow rate through an orifice inclined at an angle θ with the horizontal, and α is the kinetic angle of repose. The factor reduces to one for $\theta = 0$, and to zero for $\cos \theta = -\cos \alpha$, thus satisfying the two extreme conditions. Fig. 8 and Table II compare the

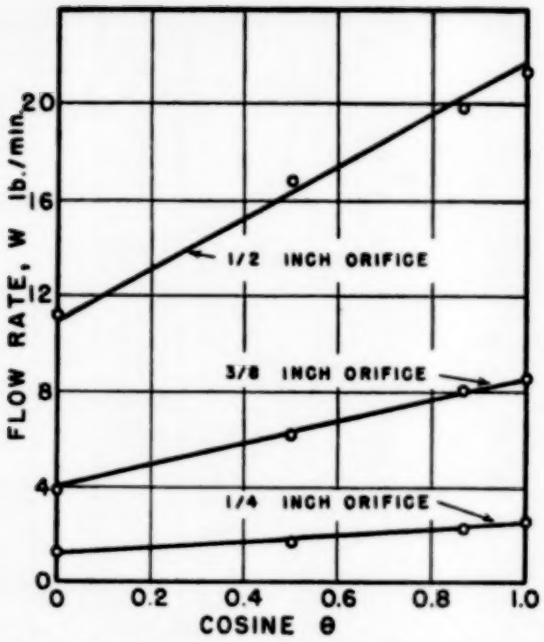

Fig. 7. Flowrate correlation of lead shot through inclined orifices.

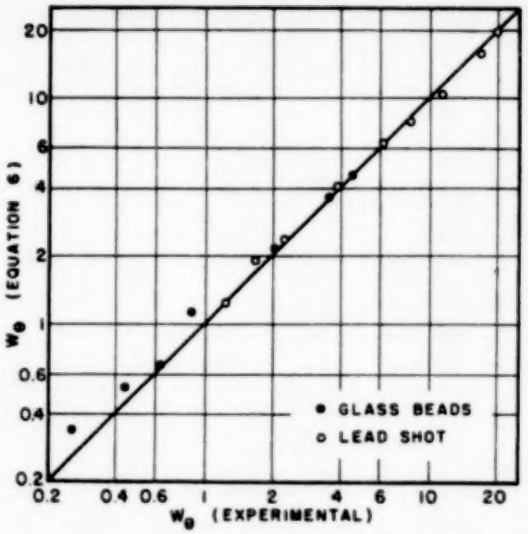

Fig. 8. Proposed flowrate correlation for inclined orifices

experimental data for inclined orifices with eq. (6). The equation appears to fit the data within the experimental error.

Thus the flow rate through an inclined orifice can be estimated from a knowledge of the flow rate through a horizontal orifice, and the inclination angle of the orifice without the need of additional empirical constants. Flow rate through the horizontal orifice can be experimental, or obtained by using Equation 5 if the orifice diameter and particle properties are known with sufficient accuracy. Gunderson's data for the flow rate through a horizontal orifice were used as the basis of comparison in Fig. 8, since the use of the nominal values of orifice diameter together with eq. (5) resulted in values for W_0 which were from 10% to 20% lower than experimental results.

It would be of interest to compare the results of previous investigators with those predicted by means of eqs. (5) and (6). No data other than Gunderson's is available for flow through inclined orifices and hence no comparison of eq. (6) with other workers' results is possible. Equation (5) for horizontal orifices can be compared with previous work, however, and the results of such comparison are summarized in Table III. The assumptions involved in these comparisons are discussed below.

Takahasi does not report values obtained experimentally, except in the form of plotted points for five materials. Values obtained from his Fig. 7 involving a thousand-fold variation in flow rate are of questionable accuracy, but have been compared with those predicted by his equation and by eq. (5) for the materials quartz sand, "iron sand," and lead shot. In lieu of a reliable particle density for "iron sand," a void fraction of 0·46 was assumed, and particle density calculated from bulk density. Internal kinetic angles of repose were obtained from Takahasi's surface angles by means of Fig. 2, for quartz and iron sand. The value for lead shot is from this work, Table I.

The agreement between experimental results and either equation is less than would be desired, but is sufficient to indicate eq. (5) represents the data about as well as does Takahasi's equation. Much of the discrepancy can be attributed to inconsistencies in the experimental data. In using these data, care was taken to avoid those results for which the ratio of particle

VOL. 4 1955

Table III. Comparison with previous work.

Material	D_o	D_p	ρ_b	ρ_p	μ_a	ϕ	*Previous Results Flow Rate, lb./min.* *Experimental*	*Predicted*	*This Work Flow Rate, lb./min.* *Experimental*	*Predicted*	*Ref.*
Quartz Sand No. 2	0·313	0·0244	84	165	0·65‡		1·12	0·84		0·74	3
	0·452						2·82	2·4		2·2	
	0·716						12·6	8·4		8·5	
	1·06						39·9	23·8		26·9	
Iron Sand No. 3	0·119	0·0059	158	292*	0·53‡		0·18	0·26		0·08	3
	0·692						10·6	32·8		5·3	
	0·92						53	69·		33·	
	1·50						188	241		137·	
Lead Shot No. 3	0·70	0·114	422	676	0·368		26·9	36		39	3
	0·766						44·7	48		51	
	1·162						178	194		172	
New Clay Catalyst	1·352	0·185		95·3	0·67			20·7	17·8	19·2	1
	2·28							97·2	82·8	89·0	
Kale Seed	0·593	0·068	41·6	68·5†	0·38‡	$180° - 2\alpha$		2·5		3·0	2
Mustard Seed	0·593	0·085	46·5	75†	0·43‡	$180° - 2\alpha$		2·4		2·6	2
Urea Pellets	0·399	0·026	47·1	83·4	0·38‡	$180° - 2\alpha$		1·4		1·4	2
Glass Beads	0·593	0·139	98	160	0·415	$180° - 2\alpha$		4·2		4·7	2
Phosphate Rock No. 1	0·196	0·017	78	200	0·59‡	$180° - 2\alpha$		0·28		0·27	2
Phosphate Rock No. 2	0·118	0·0063	80	200	0·59‡	$180° - 2\alpha$		0·095		0·062	2
Lead Shot No. 9	0·396	0·080	410	676	0·368	$180° - 2\alpha$		7·9		8·6	2
Lead Shot No. 10	0·593	0·070	408	676	0·368	$180° - 2\alpha$		28		29	2

* Based upon estimated void fraction of 0·46 and bulk density.
† Based upon estimated void fraction of 0·40 and bulk density.
‡ Obtained from Figure 2. Other values from this work.

size to orifice size, or orifice size to column size, was too great to assume independence of flow rate from these factors.

It is believed that the clay catalyst upon which eq. (1) is based is substantially the same as the new clay catalyst of this work. Properties of the latter catalyst were therefore used to enable a comparison of eq. (1) and eq. (5) with experimental results of the present work. Use of eq. (1) with bed height equal to one foot results in values about 17% high, while eq. (5) results in values about 8% high. In view of the assumptions necessary to use eq. (1), the two equation may be considered to be in agreement.

Deming and Mehring recommend their equation only for cone orifices, of cone angle ranging from 20° to 110°. Their data were obtained for 30°, 60° and 90° cone angles. The decrease in flow rate with increasing cone angle is not marked, and it would be expected that application of their equation to cone angles approaching 180°, or a horizontal orifice, would not be greatly in error. The comparison was actually made for cone angles of $180° - 2\alpha$, where α is the kinetic angle of repose. This represents approximately the natural cone formed when granular material issues through a horizontal orifice. It is reasonable to expect that flow rate would not be influenced by cone angles greater than this, and therefore eq. (2) which is that used by Deming and Mehring need be extrapolated only to this point for proper comparison with eq. (5).

There is some difficulty in making a direct comparison between their results and the present equation even if such extrapolation is justified, however. Their equation is based upon static angle of repose and bulk density of the granular solid, and they did not report values of particle density or fraction void and the kinetic angle of repose required in eq. (5). Values from Table I were therefore used for glass beads and lead shot. Kale and mustard seed densities were obtained from bulk density and an estimated void fraction of 0·4, and published densities for urea and phosphate rock were used. Internal kinetic angle of repose was estimated for these materials by means of Fig. 2. With the exception of Phosphate rock No. 2, which is considerably finer than any material used in the present work, Table III indicates the equations are in reasonable agreement at the point where they are each applicable, namely for cone angles of $180° - 2\alpha$. The values predicted from Deming and Mehring's equation are also in line with their experimental results for 30, 60 and 90 degree cone angles.

Conclusions

The mass rate of flow of granular material through circular orifices in thin flat plates can be calculated from a knowledge of a few easily measurable properties of the system. These are the orifice and particle diameters, the particle density, the angle of inclination of the orifice with the horizontal, and a kinetic angle of repose of the granular material. A device is suggested for measuring the latter value. Equation (5), or the analogous nomograph, Fig. 6, can be used to calculate flow rate through a horizontal orifice, and eq. (6) can be used to modify this for inclined orifices. For cone-bottomed containers terminating in a horizontal orifice, eq. (2) from the work of Deming and Mehring can be used up to cone angles of $180° - 2\alpha$, where α is the angle of repose. For cone angles greater than this, eq. (5) is satisfactory.

Notation

D = Diameter, inches. Subscript c refers to column, o to orifice and p to particle.
H = Height of bed above orifice, feet.
K = Intercept at $D_o = 1$ of flow rate versus orifice diameter plot.
t = Time of flow, minutes/unit volume.
V = Volume rate of flow, ft.^{3}/min. Subscript ∞ refers to flow rate through column for which $D_c/D_o \to \infty$.
W = Mass rate of flow, lb./min. No subscript or subscript o refers to flow through horizontal orifice; subscript θ to flow through inclined orifice.
α = Angle of repose. Refers to internal kinetic angle unless otherwise stated.
ϵ = Void fraction of static packed bed.
θ = Angle of inclination of orifice from horizontal.
μ = Tangent of angle of repose. Subscript 1 refers to surface static angle; 2 to surface kinetic angle, and 3 to internal kinetic angle.
ρ = Density of material lb./ft.^{3}. Subscript b refers to bulk density; p to particle density.
ϕ = Cone angle for conical orifice.

VOL. 4 1955

References

[1] Newton, R. H., Dunham, G. S. and Simpson, T. P. ; *Trans Amer. Inst Chem. Engrs*, 1945 **41** 215.

[2] Deming, W. E. and Mehring, A. L. ; *Ind. Eng. Chem.*, 1929 **21** 661.

[3] Takahasi, K. ; Institute of Physical and Chemical Research, Tokyo. *Scientific Papers*, 1934 **26** 11 (No. 540).

[4] Kennar, G. A. ; B.S. Thesis in Chemical Engineering, University of Washington (1952).

[5] Gunderson, J. M. ; B.S. Thesis in Chemical Engineering, University of Washington (1953).

Chemical Engineering Science, 1955, Vol. 4, pp. 130 to 140. Pergamon Press Ltd.

Dimensional systems and systems of units in physics with special reference to chemical engineering

Part I. The principles according to which dimensional systems and systems of units are constructed

A. KLINKENBERG

N.V. De Bataafsche Petroleum Maatschappij (Royal Dutch/Shell Group), The Hague

(*Received* 23 *January* 1955)

Summary—In Part I the principles are examined of building systems of dimensions and units in physics with special reference to the aspects for the chemical engineer.

This part provides the background for Part II which gives :

a formulation of practical rules,
a discussion of the confusion in the field, and
conclusions re advantages and disadvantages of various systems.

Résumé—Dans cette première partie, l'auteur étudie les principes rationels de l'établissmenet des systèmes de dimensions et d'unités des grandeurs physiques au point de vue spécial du GENIE CHIMIQUE.

Cette étude servira de base à une seconde partie d'écrivant :

(*a*) l'énoncé des règles pratiques.
(*b*) la discussion des confusions existant présentement dans ce domaine.
(*c*) Avantages et défauts des différents systèmes actuels.

1. INTRODUCTION

In chemical engineering much of the knowledge which authors want to convey to readers is in the form of equations. It is believed that always the ultimate aim of such equations is their use in numerical calculations be it by the author or by the reader.

It is the purpose of this paper to examine how this aim may be reached with the least risk of making mistakes.

A well-known text book [1], page 29, says :

> " The data of the chemical engineer will often be found in various systems of units and he must be able to disentangle them. The burden of straight thinking is upon him and he must be able to avoid the confusion induced by the terminology employed by brother engineers."

This quotation only covers the reader's aspect. The crux, however, lies with his " brother chemical engineer," the author. While the philosophy of this paper is to allow the author the use of any system of units – disallowing of course any haphazard assembly of units – the point is equally strongly pressed that the reader has the right to see the system of units used correctly.

This latter point carries added weight in view of the circumstance that the user of an equation often has no time to go through its complete derivation. In fact, he glances through the article, until he finds a combination of the right symbols, and he wants to use that equation rightaway, possibly with units of his own choice.

For the above to be possible without undue effort it is necessary that dimensions and units should be well understood, handled correctly and indicated clearly.

The following text gives in Part I a description of the principles used in building up systems of dimensions in current use. It has been tried to give this description with the least amount of arithmetic ; for this reason, some statements may appear to be without proof. A rigid background may be obtained with the aid of works by BRIDGMAN [2], FOCKEN [3] and others.

In Part II a number of practical rules are formulated for the use of authors and readers of papers and reports in which calculations of a physical nature are carried out. These are followed by a critical discussion of literature quotations.

It is clear that the above aims can be reached much more efficiently if (1) symbols are standardized; (2) everyone uses the same dimensional formulae and units. The first of these points will not be touched. The second would have following obvious advantages: no attention need be devoted to mastering several systems; no conversion factors are required and no actual work of conversion need be done; a better feeling can be developed for the numerical values of physical magnitudes* if they are always expressed in the same units.

In order to assist in the choice of the most suitable system a summary (Part II, § 5) has been prepared of the advantages and disadvantages of various systems as derived from *a priori* considerations and as noted in the critical discussion of the literature.

2. Quantities Occurring in Equations

The equations, seen as relations between numbers

One way of looking at equations is that they represent certain mathematical relations between numbers.

These numbers may be of various types, namely:

(*a*) Simple numerical factors (definitional constants according to Guggenheim [4]).

(*b*) Numbers expressing the size of a physical magnitude and represented by a letter symbol. Such letter symbols stand for the ratio of the size of a physical magnitude to the size of the corresponding unit.

(*c*) Numbers expressing the size of a physical magnitude and given as such, i.e., as a numeric, equal to the ratio mentioned under (*b*).

(*d*) So-called dimensional constants, represented by a letter symbol or by a number.

These arise from the fact that the units for certain physical quantities can be derived in more than one way from the units for the quantities assumed fundamental.

A few simple cases will provide examples for the above four types of factors.

1. *Free fall without initial velocity*

If path is measured in metres and time in seconds, we may write:

$$s = \frac{9{\cdot}8}{2} t^2 = 4{\cdot}9\, t^2 \qquad (1)$$

In this equation we find:

(*a*) a numerical factor $\frac{1}{2}$;

(*b*) sizes of physical magnitudes "path" and "time," expressed by letter symbols s and t;

(*c*) size of physical magnitude "acceleration," expressed by numerical value 9·8;

(*d*) no dimensional constant.

2. *Shear stress in a liquid*

The relation between shear stress τ and velocity gradient du/dy in a fluid is represented in a certain case by:

$$g_c\, \tau = \eta \frac{du}{dy} \qquad (2)$$

when τ is measured in lb._f/sq.ft.*
η (= viscosity) in lb._m/ft.sec.*
u (= velocity) in ft./sec.
y (= a coordinate) in ft.

Besides sizes of physical magnitudes (see para. (*b*) above) the equation contains a dimensional constant g_c of numerical value 32·2.

The occurrence of this constant is due to the existence of alternate routes in deriving units. We might have defined the poundal (force acting on 1 lb. mass with an acceleration of 1 ft./sec.^{2}) and used this unit in the equation without a factor g_c. However, we have chosen the lb. force (= force acting on a 1 lb. mass with an accelera-

* Following Fockes [3], length is a physical quantity, and the length of a particular object is a physical magnitude.

* lb._f = pound force; lb._m = pound mass.

tion of $g = 32{\cdot}2$ ft./sec.^{2}) instead. Since the number of lbs. force is $\frac{1}{32{\cdot}2}$ the number of poundals, the factor $g_c = 32{\cdot}2$ must then be included.

3. *The first law of thermodynamics*

If energy is expressed in two ways, viz. as work in mechanical units and as heat in heat units, the mechanical heat equivalent enters as a dimensional constant.

Of the four types of numbers that may occur in equations, one, viz. type (*c*), is often undesirable. We may discuss this point by taking the equation (1), $s = 4{\cdot}9\,t^2$ as an example. This form of equation has the advantage of being immediately usable for anyone employing m and sec. as his fundamental units, whereas with $s = \frac{1}{2}\,gt^2$ the substitution of $g = 9{\cdot}8$ is still needed. On the other hand equation (1) has the great disadvantage of requiring conversion if it is to be used with s and t expressed in units other than m and sec.

For the generality of the treatment it is therefore considered advisable to work as long as possible in letter symbols, to replace the constants such as g and various physical properties by their numerical values only immediately prior to the use of the equation for a numerical calculation and from that point onward, always to state precisely what units are to be used.

Thus :

$$s = 4{\cdot}9\,t^2 \text{ (units : m and sec.)}$$

exactly as one would say

$$t = 20°\text{C}$$

and never simply

$$t = 20$$

The equations containing nothing but purely mathematical numbers (*a*) and letter symbols representing the sizes of physical magnitudes (*b*) or the values of dimensional constants (*d*) are called complete. They are invariant for changes in the size of the units. Indeed, one should wish the description of the laws of nature to be independent of our choice of units. It is, however, to be noted that such invariance can be reached with regard to changes in *size* of units and fundamental units, but not with regard to changes in *type* (see examples 2 and 3).

The equations, seen as relations between physical magnitudes

So far, all symbols stood for numbers. One may also look at the symbols differently and consider them to represent the physical magnitudes themselves. This, however, is the subject of violent attack by some authors, who maintain that it is impossible to multiply or divide physical magnitudes.

The stand taken here is that it is perfectly legitimate and very convenient to do so.

This simply means that the concept of multiplication is given a wider scope than it has in arithmetic.

Even in pure mathematics this procedure is known. When making the vector product $\bar{c} = \bar{a} \times \bar{b}$, each vector $\bar{v}$ is considered to be the product of a numerical value v and a unit vector v_1. The equation

$$c\,c_1 = a\,\bar{a}_1 \times b\,\bar{b}_1 \tag{3}$$

then falls apart in the two equations

$$c = ab \tag{3a}$$

and

$$\bar{c}_1 = \bar{a}_1 \times \bar{b}_1 \tag{3b}$$

It might seem astonishing to derive two equations from one. This point will be clarified by an example from physics:

Since a body in uniform motion at 10 m/sec. in 1 hr. covers a path of 36 km one may say :

$$36 \text{ km} = 10 \text{ m/sec.} \times 1 \text{ hr.}$$

This statement is evidently highly impractical. It may be made practical in two ways, viz. by writing :

Firstly :

$$36000 \text{ m} = 10 \text{ m/sec.} \times 3600 \text{ sec.}$$

Here the equation falls apart in two :

$$36000 = 10 \times 3600$$

and

$$1 \text{ m} = 1 \text{ m/sec.} \times 1 \text{ sec.}$$

VOL. 4 1955

We have achieved this by relating the unit of velocity to the units of length and time.

Secondly :

$$36 \text{ km} = 10 \text{ m/sec.} \times 1 \text{ hr.} \times 3{\cdot}6 \frac{\text{km.sec.}}{\text{m.hr.}}$$

The added factor is a dimensional constant.

Again, both the numbers and the units are in order.

In either case, by considering every physical magnitude to be the product of a numerical value and a unit, we have obtained the possibility to use the equation in two ways, namely to calculate numerical values and to carry out a check on dimensional homogeneity.

The conversion into other units by varying the size of the fundamental units also becomes very simple, viz. :

$$36 \frac{\text{km}}{\text{hr.}} = 36 \frac{1000 \text{ m}}{3600 \text{ sec.}} = 10 \frac{\text{m}}{\text{sec.}}$$

There is no risk of introducing conversion factors the wrong way round.

The interpretation of the equations as relations between physical magnitudes is used or advocated, amongst others, by CORNELIVS and HAMAKER [5], FLEISCHMANN [6], GUGGENHEIM [4], PAGE [7], POHL [8], and THORNE and WALSHAW [9].

A difficulty arises if the equation would contain logarithms of physical magnitudes. On closer thought, it is seen only to contain logarithms of ratios, i.e. differences of logarithms. However, one such logarithm may be visible and the other concealed in an integration constant (examples : integrated Clapeyron equation ; Arrhenius equation ; entropy of an ideal gas).

This forces one, if one writes the equation in the usual form, either to accept logarithms of physical magnitudes and units or in this case to use numerical values only.

The author is inclined not to take this difficulty too seriously and to argue that, whatever illogical or physically impossible is done, it is done twice and cancels out. Reference is made to BRIDGMAN [2] and FOCKEN [3], page 43.

Of the afore-mentioned two methods of obtaining dimensional homogeneity, the first by far is the most common, but it is absolutely essential for the understanding of systems of units that the second method is well recognized.

So far, we made a direct jump to units, to be distinguished as fundamental units (in the first example : m and sec.) and derived units (in the first example : m/sec.).

In order to write and read complete equations in letter form, however, there need be no more than agreement on fundamental quantities, i.e. on *types* of fundamental units to be used (length and time in the first example), and agreement on certain conventions that fix numerical constants.

Such conventions are, for example : deriving the unit of area from a square with unit side and not from a circle with unit diameter ; deriving the Reynolds group from a pipe diameter and not from a radius ; choosing between placing a factor $1/4\pi$ in the formula for the electrical capacity of a plane condenser (in the cgs system) or a factor 4π in that for the capacity of a sphere (" rationalization " as applied in the practical system).

The matter of *sizes* of fundamental units only arises at a later stage when numerical values are substituted and the resultant equations are no longer complete.

These two steps should therefore in the derivation of equations be made separately.

3. SOME PRINCIPLES OF CHOOSING TYPES OF FUNDAMENTAL UNITS

The problem of units in physics and engineering is sometimes considered to involve primarily a choice between "the" metric and "the" English system.

The present discussion will underline that this is a serious understatement. It should be noted :

1. That the matter of choice of fundamental quantities (*types* of fundamental units) is much deeper rooted and requires more insight than the matter of the choice of *size* of fundamental units (see, e.g., FLEISCHMANN [24]) ;
2. That even for given fundamental quantities the metric as well as the English system allow various alternatives (cm-m ; g-kg ; in.-ft. ; sec.-hr.) all of which are in use.

The above example of movement at uniform velocity showed two ways of obtaining a complete equation :

Firstly : by relating the unit of velocity to the units of length and time.

Secondly : by introducing a dimensional constant without relating the unit of velocity to the units of length and time.

For this example every one agrees that the first method is to be preferred, since it is the simpler.

In continuing in this manner to relate derived quantities to fundamental quantities one builds up a system of dimensions.

The so-called dimensional formulae, such as

$$\text{velocity} = [\,L\,T^{-1}]$$

are nothing but a useful short-hand notation to see how this is done.

The statement

$$\text{unit of velocity} = \text{m.sec.}^{-1}$$

serves the same purpose. In view of § 2 this statement, however, at this point introduces an unnecessary limitation.

It is preferred to call $[L\,T^{-1}]$ the " dimensional formulae " and not the " dimension." The latter term should be reserved for the set of exponents. Velocity thus has the dimensions $+1$, 0 and -1 in length, mass and time. In this way a dimensionless quantity has dimensions zero in all fundamental quantities, but its dimensional formula is unity.

This principle of avoiding dimensional constants when carried through further and further, all through physics, finally defeats itself.

It may be argued that one has gone too far already in the cgs system.

In this system all electric and magnetic quantities are derived from length, mass and time, with the consequent appearance of weird dimensional formulae such as

$$\text{electric charge in electrostatic system} = [L^{3/2}\,M^{1/2}\,T^{-1}].$$

Such dimensional formulae do not, as it is sometimes believed, betray the deepest secrets of nature. Instead they are rather confusing and they have been an obstacle to generations of physicists. It will be seen that a system with 4 fundamental units is more convenient.

The argument may be carried further to extremes and in order to bring out very clearly the arbitrariness of all systems of dimensions, this will, in the following, be done.

The starting point is that the cgs electric and magnetic units are derivable in two ways :

via Coulomb's Law for the electric attraction (electrostatic units) ;

via the magnetic analogon of this Law (electromagnetic units).

Accordingly, when both routes are being used, a dimensional constant will occur.

Such a constant is therefore met :

in Coulomb's Law when using electromagnetic units of charge ;

in the Law for attraction of magnetic poles when using electrostatic units of pole strength ;

in Maxwell's Law, which relates the magnetic field strength H to the current i producing it, when H is expressed in electromagnetic units and i in electrostatic units (Gauss' system of units).

These dimensional constants are equal to the velocity of light c or some power of it. They could be removed by making the velocity of light dimensionally and numerically equal to 1. This would mean giving up either the cm or the sec., e.g., introducing 3×10^{10} cm as a unit of length.

This might be convenient in the theory of relativity, e.g. in describing the energy liberated in atomic fission (the energy mc^2 is now measured in units of mass) or in astronomy (light seconds simply become seconds), but it is decidedly impractical in general physics.

A further reduction in fundamental quantities would be possible by eliminating the gravitation constant in Newton's Law for attraction of masses, by which, if one sticks to the second, one loses the gram too.

This would leave us with one fundamental unit

VOL. 4 1955

and with highly impractical derived units. Moreover dimensional formulae lose their usefulness, since they then provide less insight on relations between physical quantities and checks on dimensional homogeneity become less powerful (note coincidences such as capacity (e.s. cgs units) = length).

A further difficulty is that dimensional analysis, when carried out with too few fundamental units, gives too many dimensionless groups.

A discussion on the latitude in the number of fundamental units to be used is given by GUGGENHEIM [4].

Since it is usually avoided to introduce dimensional constants in equations relating quantities belonging to the same field of physics, the dimensional constants, whenever occurring, are normally found at the junctions of various fields, i.e., in some equations of great fundamental importance, such as

Newton's Gravitational Law, Newton's Law of Acceleration } joining kinetics and dynamics

First Law of Thermodynamics, joining mechanics and heat

Coulomb's Law, joining mechanics and electricity

Magnetic Attraction Law, joining mechanics and magnetism

Maxwell's Law, joining electricity and magnetism

The law of gravitation keeps its dimensional constant in all systems of dimensions in practical use.

The way of handling the law of acceleration is crucial for the dimensions in mechanics and hence forms the basis of all dimensions and units in general physics and engineering.

For this reason Newton's Law of acceleration will be discussed first.

4. The Methods of Using Newton's Law of Acceleration in Building a System of Dimensions for Mechanics

Newton's Second Law will be used in the form of the statement that force is proportional to mass and to acceleration.

Newton's Law without dimensional constant

If used without a dimensional constant Newton's Law becomes

$$F = ma \text{ (static and dynamic systems)} \qquad (4)$$

Since there are obvious stringent reasons always to relate the acceleration to the fundamental quantities of length and time, there are two possibilities left:

dynamic systems, sometimes called absolute systems :

> mass m, length L and time T are fundamental; force F is a derived quantity with dimensional formula : $F = [MLT^{-2}]$.*

static systems, sometimes called gravitational, technical or engineering systems :

> force F, length L and time T are fundamental; mass m is a derived quantity with dimensional formula $m = [FL^{-1}T^{2}]$.

Each of these principles can be used with grams, kilograms or pounds as mass units or as force units, with cm, m or ft. as units of length and with seconds or hours as units of time, in various combinations.

Newton's Law with a dimensional constant

If used *with* a dimensional constant, Newton's Second Law reads :

$$g_c F = ma \text{ (Engl. Engin. system, new version)} \qquad (5)$$

The English Engineering system† (new version) is based on the fundamental quantities of force (unit : $lb._f$), mass (unit : $lb._m$), length (unit : ft.) and time (unit : either sec. or hr.) with the dimensional constant

$$g_c = [M L T^{-2} F^{-1}] \text{ (Engl. Engin. system, new version)} \qquad (6)$$

Since the same quantity of matter serves to define the units of both force and mass, application of eq. (5) to free fall shows that g_c is numerically equal to g.

---

* Capital M is used for mass in dimensional formulae.

† Name adapted from [1], page 28 ; however, the "British Engineering system" discussed by COULSON and RICHARDSON [10] page 2, is a static system.

Once the use of four fundamental quantities has been decided upon, it is logically impossible to relate one of them to the three others.

The quantities closely associated with force are naturally expressed in units derived from $lb._f$ (e.g. work, power, pressure, shear stress τ), those more closely related to mass in units derived from $lb._m$ (density ρ). This segregation, however, is somewhat arbitrary. Regarding viscosity a choice must be made in order that one knows whether the g_c should be placed in $\tau = \eta \frac{dv}{dx}$ or in $\eta = \rho\nu$. It is advisable to relate the viscosity to the $lb._m$ in order also to keep the definition of the Reynolds group unchanged. It might be safe to distinguish the two definitions by subscripts (η_f and η_m).

If potential energy is expressed in $ft.lb._f$ and kinetic energy in $lb._m ft.^2 sec.^{-2}$, they will have a factor g_c between them. Also, in the First Law of Thermodynamics it should be remembered, which of these energy units serves in defining the mechanical equivalent of heat.

These examples can no doubt be multiplied.

Part II presents an example (number A 10), where the unit for pressure is derived from $lb._f$ and the unit for shear stress from $lb._m$.

The use of this dimensional system with metric units is very rare. E. SCHMIDT [11] mentions the desirability to use it. He uses the symbol kg for the kg_m only and introduces kp (= kilopond) for the kg_f. The unit of energy is kpm and not $kg\ m^2\ sec.^{-2}$, so that the equality of mechanical and electrical units of energy is lost. Since this system is not (yet) in use, SCHMIDT carries on in technical, i.e. FLT units.

The English Engineering system (new version) has developed from an older version, where the two fundamental quantities of force and mass and their units were not kept distinguished.

In this old version both force and mass are given the dimensional formula [M] and the unit is the pound – without any subscript. The dimensional constant then becomes dimensionally and numerically equal to g, i.e. :

$$gF = ma \quad \text{(Engl. Engin. system, old version)} \quad (7)$$

It is impossible to say that the old version is incorrect. It can no doubt be handled correctly. However, the use of the same pound for both force and mass goes at the expense of clarity, it makes dimensional checks and dimensional analysis less powerful and it must have been a source for much confusion. This has no doubt induced the development of the new version.

The old version is – or recently was – still in use by many well-known chemical engineers, e.g. LEVA [12] and WILHELM [13] in the U.S. and PRATT [14] in the U.K.

The new version is employed at the Mass. Inst. Technology (see e.g. MCADAMS [15]), by the Dupont Eng. Expt. Station, whose Dr. T. H. CHILTON is an ardent defender, and by Shell Development Co.

WALKER, LEWIS, MCADAMS and GILLILAND [1], page 29, after defining English dynamical (= absolute), statical (= gravitational) and engineering units (i.e. old version) said in 1937 :

> "This text will express final equations in engineering units but wherever ambiguity can arise will distinguish between pound mass and pound force. It is easier to make derivations in absolute units (e.g. mass in pounds, force in poundals) and transform the final expressions into engineering units."

Stronger condemnation of the engineering system cannot be imagined. It is felt, however, that by distinguishing $lb._m$ and $lb._f$, the greatest stumbleblock has since been removed.

WORELL [16] believes to have an argument that $F = ma$ is right and $g_c F = ma$ is wrong. He says that the relation differs from all others, which only express proportionalities, in that F is ma.

The tables overleaf gives a survey of some important units in the most important systems derived according to the four principles described.

Special Subjects

The molal units

In many fields (thermodynamics, kinetic theory, stoichiometry) there is a need for a molal mass unit.

It is recommended to introduce [Mol] as an additional fundamental quantity in dimensional formulae and to regard the molecular weight M as a dimensional quantity :

VOL. 4 1955

$$\mathbf{M} = [\mathbf{M\,Mol^{-1}}] \qquad (8)$$

(see footnote § 3 on **M** in dimensional formulae).

The units for the quantity Mol are mol, kmol and lbmol.

Dynamic Systems

	cgs System	MKS *Practical System**	*British Dynamic System*
Fundamental Units			
length	cm	m	ft.
mass[1]	g_m	kg_m	$lb._m$
time	sec.	sec.	sec.[2]
Derived Units			
force	g_m cm sec^{-2} (= dyne)	kg_m m sec^{-2} (= newton)	$lb._m$ ft. sec.$^{-2}$ (= poundal)
work	g_m cm^2 sec.$^{-2}$ (= erg)	kg_m m^2 sec.$^{-2}$ (= joule)	$lb._m$ ft.^{2} sec.$^{-2}$ (= ft.poundal)
density	g_m cm^{-3}	kg_m m^{-3}	$lb._m$ ft.$^{-3}$
sp. weight	$g_m$cm^{-2}sec.$^{-2}$	kg_m m^{-2} sec.$^{-2}$	$lb._m$ft.$^{-2}$sec.$^{-2}$
dyn. viscosity	$g_m$cm^{-1}sec.$^{-1}$ (= poise)	kg_m m^{-1} sec.$^{-1}$	$lb._m$ft.$^{-1}$sec.$^{-1}$

(1) The user of a dynamic system will usually omit the subscript m. It is added here for extra security.

(2) Hours may also be used.

* *Warning* : The abbreviation " MKS System " is in use for both the practical and the technical metric system.

Static Systems

	Small Metric Static	*Technical Metric*	*British Static*
Fundamental Units			
length	cm	m	ft.
force[1]	g_f	kg_f	$lb._f$
time	sec.	sec.	sec.[2]
Derived units			
mass	$g_f$cm^{-1} sec.^{2}	kg_f m^{-1} sec.^{2}	lb_f ft.$^{-1}$ sec.^{2} (= slug)
work	g_f cm	kg_f m	ft. $lb._f$
density	g_f cm^{-4} sec.^{2}	kg_f m^{-4} sec.^{2}	$lb._f$ ft.$^{-4}$ sec.^{2}
sp. weight	g_f cm^{-3}	kg_f m^{-3}	$lb._f$ ft.$^{-3}$
dyn. viscosity	g_f cm^{-2} sec.	kg_f m^{-2} sec.	$lb._f$ ft.$^{-2}$ sec.

English Engineering System

	New Version	*Old Version*
Fundamental Units		
length	ft.	ft.
mass	$lb._m$	lb.
time	sec.[3]	sec.[3]
force	$lb._f$	lb.
Derived Units		
work	ft. $lb._f$	ft. lb.
density	$lb._m$ ft.$^{-3}$	lb. ft.$^{-3}$
sp. weight	$lb._f$ ft.$^{-3}$	$lb._f$ ft.$^{-3}$
pressure	$lb._f$ ft.$^{-2}$	lb. ft.$^{-2}$
dyn. viscosity, η_m	$lb._m$ ft.$^{-1}$ sec.$^{-1}$	lb. ft.$^{-1}$ sec.$^{-1}$
or alternative : η_f	$lb._f$ ft.$^{-2}$ sec.	lb. ft.$^{-2}$ sec.
dimensional constant[3]	$g_c = 32{\cdot}2 \cdot \frac{lb._m ft.}{lb._f sec.^2}$	$g = 32{\cdot}2\ \frac{ft.}{sec.^2}$

(1) The user of a static system will usually omit the subscript f.

(2) Hours may also be used.

(3) *Note*: Hours are also frequently used, the numerical value of g_c or g thus becoming $4{\cdot}17 \times 10^8$.

AVOGADRO's number N now becomes a physical quantity instead of a pure number :

$$N = 6{\cdot}06 \times 10^{23}\ \text{mol}^{-1} = 6{\cdot}06 \times 10^{26}\ \text{kmol}^{-1} = 2{\cdot}75 \times 10^{26}\ \text{lb.mol}^{-1}$$

This procedure is very convenient in dimensional checks. For instance, COULSON and RICHARDSON [10], p. 248, give the mean velocity of gas molecules as $\sqrt{8\,\overline{RT}/\pi}$.* Obviously a factor **M** has been omitted in the denominator. If R is expressed in mechanical work per unit of mass and unit of temperature, $R = [\mathrm{L^2\,T^{-2}}\Theta^{-1}]$, this omission does not show, but with $R = [\mathrm{ML^2\,T^{-2}\,Mol^{-1}}\Theta^{-1}]$ it is found immediately.

Specific mass (or density) and specific weight (or specific gravity)

If density is denoted by ρ and specific gravity by γ, the hydrostatic pressure at depth h is in both the dynamic and the static systems given by the two equations

$$p = \rho g h \qquad (9)$$

* R being defined as the *universal* gas constant.

$$p = \gamma h \qquad (10)$$

However, the first definition is preferred in dynamic systems, where ρ has a simple meaning and the second in static systems.

Similarly the kinetic energy will be written as $\frac{1}{2}\rho v^2$ in dynamic and $\frac{1}{2}\frac{\gamma}{g}v^2$ in static systems, although these expressions are correct in both groups of systems.

It is thus seen that in static systems the preferred equation contains g when gravity has no influence and vice versa.

Specific quantities based on mass or weight

Attention is drawn to the fact that specific heat, entropy, internal energy, etc., are referred to unit mass in dynamic systems and to unit force in static systems.

Thus, these quantities in the two groups of systems differ dimensionally, although the numerical values are equal and the symbols also the same.

Due to this difference in the definitions some equations read differently in the two systems. An example is the definition of the dimensionless group named after PRANDTL.

$$Pr = \frac{\eta c_p}{\lambda} \text{ (dynamic)} \qquad Pr = \frac{\eta c_p g}{\lambda} \text{ (static)}$$

where

$$\eta = [ML^{-1}T^{-1}] \qquad \eta = [FL^{-2}T]$$
$$c_p = [QM^{-1}\Theta^{-1}] \qquad c_p = [QF^{-1}\Theta^{-1}]$$
$$\lambda = [QL^{-1}T^{-1}\Theta^{-1}] \qquad \lambda = [QL^{-1}T^{-1}\Theta^{-1}]$$

The extra factor is g, not g_c.

5. EXTENSION TO THE OTHER FIELDS OF PHYSICS

Heat

When it is tried to extend the process of deriving dimensional formulae of physical quantities to the field of heat, the difficulty is met that more than one unknown occurs simultaneously so that it is impossible to derive the units to be used in this field without additional assumptions (RÜCKER [17]).

In all equations that might serve for such derivation heat is equated to a product of temperature with a quantity such as the gas constant, entropy, specific heat or thermal conductivity and possibly with purely mechanical quantities (mass, area).

Since there are three unknowns, two assumptions may be made, when the dimensions of the third quantity can be found.

The methods in practical use have one assumption in common, i.e. temperature is introduced as a new fundamental quantity. This is necessary in order to be allowed to use the °C or °F.

The other assumption is :

1. Heat is a fundamental quantity.
2. Heat is expressed in the units of mechanical energy.
3. The specific heat is made dimensionless (its dimensions are suppressed).

A suggestion how to derive temperature from mechanical quantities was given by RÜCKER [17]: "The unit of temperature is that necessary to produce an increase of 1 erg in the mean total energy of translation of the molecules contained in 1 cm³ of gas at 0°C and 1 atm." Here the two assumptions are : heat expressed in mechanical units ; suppression of the dimensions of R.

Ad 1

The first method is followed when the cgs, technical metric and various British systems are extended with calorie plus °C, kcal plus °C and BTU (or centigrade heat unit) plus °F or °C respectively. The mechanical equivalent of heat J is a dimensional constant.

Ad 2

The second method is followed when the MKS system is extended with the °C. The unit of heat, joule, is equal to the mechanical unit of work, newton metre. This method has the advantage of not requiring the mechanical equivalent of heat. The unit of heat, joule, is also the unit in which electrical energy is measured and for this reason it is practical to use it in calorimetry. The Royal Society has announced [18] preference for the joule over the calorie in scientific work.

Ad 3

In the third method the specific heat of water is

made not only numerically equal to unity – by the definition of calorie and BTU – but also dimensionally.

Thus :

heat	$= [M\Theta]$
specific entropy	$= [1]$
thermal conductivity	$= [ML^{-1}T^{-1}]$

This method is followed by RÜCKER [17], INGERSOLL and ZOBEL [19], page 6, and by COULSON and RICHARDSON [10], page 3.

In view of the arbitrariness involved in every choice of fundamental units it cannot be said that this method should be incorrect. In fact, making the specific heat dimensionless, and unity for water at 15°C is not very much more arbitrary than making the dielectric constant dimensionless and unity for vacuum (in the cgs electrostatic units).

However, it is felt that by this method dimensional formulae lose much of their clarity to workers already used to other systems. While it cannot be denied that the method may be useful in heat transfer, it certainly is in the way if we see the use of one coherent system of units for the entire field of physics and engineering as the ultimate aim.

Electricity and magnetism

Here, too, the difficulty arises that the units cannot be derived from purely mechanical units without an additional assumption. Coulomb's Law, for instance, containing *two* electrical quantities, charge and dielectric constant.

The two ways followed are :

suppression of the dimensions of one electrical quantity :

in cgs e.s. system (dielectric constant),

in cgs e.m. system (magnetic permeability).

making one electrical quantity fundamental :

in practical system.

For the cgs system reference is made to the discussion, p. 134.

In the practical system both the dielectric constant ϵ and the magnetic permeability μ are no longer pure numbers. Each electrical unit can be derived in one manner only. No electrical unit can be derived from mechanical units only (see POHL [8]).

Coulomb's Laws for electrostatic and for magnetic repulsion in vacuo in the practical system are written

$$F = \frac{e_1 e_2}{4\pi\epsilon_0 r^2} \qquad F = \frac{\Phi_1 \Phi_2}{4\pi\mu_0 r^2}$$

with e_1, e_2, electric charges, and ϕ_1, ϕ_2, magnetic fluxes.

Whether ϵ_0 and μ_0 are interpreted as dimensional constants or properties of the vacuum is probably a matter of taste.

ϵ_0 = permittivity = dielectric constant of empty space =

$$\frac{10^7}{4\pi\,(3 \times 10^8)^2}\,\frac{\text{A sec.}}{\text{V m}} = 8{\cdot}853 \times 10^{-12}\,\frac{\text{A sec.}}{\text{V m}}$$

μ_0 = permeability = induction constant of empty space =

$$4\pi\ 10^{-7}\,\frac{\text{V sec.}}{\text{A m}}$$

with

$$\frac{1}{\epsilon_0\,\mu_0} = (3 \times 10^8\ \text{m/sec.})^2 = c^2$$

The factor 4π is introduced for the purpose of rationalization (see page 133).

From the user's point of view it is immaterial which extra electrical quantity is used in fixing the practical units. Proposals are : ohm, ampère (actually preferred) and $\mu_0 = 4\pi \times 10^{-7}\,\frac{\text{V sec.}}{\text{A m}}$.

Dimensional formulae and units, expressed in fundamental units may become very cumbersome. WILLIAMS [20] in a treatise on the practical system, e.g. states the unit of ϵ_0 to be $m^{-3}\,kg^{-1}\,sec.^4\,A^2$.

Units, the physical significance of which is easy to grasp, are obtained when expressing them in terms of V, A, m and sec. [21, 22].

The units for ϵ_0 and μ_0 as given above are seen to be symmetrical in structure and convert into each other if V and A are interchanged. This very convenient symmetry is found throughout electrostatics and magnetism.

Compare :	*Unit*		*Unit*
electric field strength E	$\frac{V}{m}$	magnetic induction, B	$\frac{V\ sec.}{m^2}$
dielectric displacement, D	$\frac{A\ sec.}{m^2}$	inductance, L	$\frac{V\ sec.}{A}$
capacity, C	$\frac{A\ sec.}{V}$		
with			
magnetic field strength, H	$\frac{A}{m}$		

For further literature on the practical system reference is made to : VAN DIJCK [22], Netherlands Standardization Sheets [21], POHL [23], and CORNELIUS and HAMAKER [5].

REFERENCES FOR PART I

[1] WALKER, W. H., LEWIS, W. K., MCADAMS, W. H. and GILLILAND, E. R.; *Principles of Chemical Engineering*, 3rd Ed., 1937.

[2] BRIDGMAN, P. W.; *Dimensional Analysis*, 1931.

[3] FOCKEN, C. M.; *Dimensional Methods and their Application*, 1953.

[4] GUGGENHEIM, E. A.; *Phil. Mag.* 1942 (VII) **33** 479.

[5] CORNELIUS, P. and HAMAKER, H. C.; *Philips Res. Reports* 1949 **4** 123.

[6] FLEISCHMANN, R.; *Z. f. Physik* 1951 **129** 377.

[7] PAGE, C. H.; *Amer. J. Phys.* 1952 **20** 1.

[8] POHL, R. W.; *Naturwiss.* 1951 **38** 247.

[9] THORNE, F. W. and WALSHAW, A. C.; *Engineering Units and the Stroud Convention*, 1934.

[10] COULSON, J. M. and RICHARDSON, J. F.; *Chemical Engineering*, Vol. I. Fluid Flow, Heat Transfer and Mass Transfer, 1954.

[11] SCHMIDT, E.; *Einführung in die technische Thermodynamik*, 4th Ed., 1950.

[12] LEVA, M., WEINTRAUB, M. and GRUMMER, M.; *Chem. Eng. Progress* 1949 **45** 563.

[13] WILHELM, R. H. and KWAUK, M.; *Chem. Eng. Progress* 1948 **44** 201.

[14] DELL, F. R. and PRATT, H. R. C.; *Trans. Inst. Chem. Engrs. (London)* 1951 **29** 89.

[15] MCADAMS, W. H.; *Heat Transfer*, 2nd Ed., 1942.

[16] WORELL, F. T.; *Amer. J. Phys.* 1952 **20** 456.

[17] RÜCKER, A. W.; *Phil. Mag.* (V) 1889 **27** 104.

[18] SIR CHARLES DARWIN; *Memorandum on the Unit of Heat*, April 2, 1950. See *J. Inst. Petr.* 1951 **37** 158.

[19] INGERSOLL, L. R. and ZOBEL, O. J.; *Heat Conduction*, 1948.

[20] WILLIAMS, D.; *Physics Today* 1954 (April) **7** (No. 4) 8.

[21] Hoofdcommissie voor de Normalisatie in Nederland, Standardization sheets " Het Practische Eenhedenstelsel " 1953
N 930 General Introduction
N 1221 Geometry and Kinematics
N 1222 Statics and Dynamics
N 1223 Electricity and Magnetism
N 1224 Heat and Radiation (Light and Sound).

[22] VAN DIJCK, W. J. D.; *Over het nut van één maatstelsel, het practische maatstelsel* (The Hague, 1948), issued by N.V. De Bataafsche Petroleum Maatschappij.

[23] POHL, R. W.; *Einführung in die Physik*, Erster Band, Mechanik, Akustik und Wärmelehre
Zweiter Band, Elektrizitätslehre
Dritter Band, Optik.

[24] FLEISCHMANN, R.; *Naturwiss.* 1954 **41** 131.

Chemical Engineering Science, 1955, Vol. 4, pp. 141 to 148. Pergamon Press Ltd.

On the steady state fractionation of multicomponent and complex mixtures in an ideal cascade

Part 3. Discussion of the numerical method of calculation

ANDREAS ACRIVOS* and NEAL R. AMUNDSON**

(*Received* 26 *January* 1955)

Summary—In this paper the formulae necessary for rectification calculations on complex mixtures are summarized and developed for numerical computation. These formulae involve the computation of improper integrals for which a method of calculation is developed. A numerical example is considered in some detail since these calculations are not of a routine nature. The calculations were carried out in the I.B.M. 602 A. Calculating Punch. The plate by plate method is also considered.

Résumé—Dans cet article, les auteurs ont résumés et développés, en vue d'applications numériques, les formules nécessaires au calcul de la rectification dans le cas de mélanges complexes. Ces formules impliquent le calcul d'intégrales impropres pour lesquelles ils exposent une méthode de calcul. Ils étudient en détail un exemple numérique puisque de tels calculs ne se rencontrent pas couramment. Les calculs ont été publiés dans le "I.B.M. 602 A. Calculating Punch." Les auteurs considèrent aussi la méthode "plateau par plateau."

RESUME AND FURTHER DEVELOPMENT OF NECESSARY FORMULAE

In the previous two parts the general theory of the distillation of complex mixtures has been developed for an ideal cascade. Formulae were developed, under the usual simplifying assumptions, which enabled one to make computations involving the number of stages required or the compositions attained by either a plate by plate method or by means of a formula in closed form involving some improper integrals. In order that reference to the previous papers be minimised the necessary formulae are summarized here.

If $x_n(p)$ and $y_n(p)$ are the distribution functions of the liquid and vapour, respectively, from the nth stage, then

$$\int_0^\infty x_n(p)\,dp = 1$$

$$\int_0^\infty y_n(p)\,dp = 1$$

A mass balance around the top n stages gives

$$y_{n+1}(p) = \frac{R}{R+1}\,x_n(p) + \frac{x_0(p)}{R+1} \tag{1}$$

while the equilibrium relation is assumed to be, for continuous mixtures,

$$x_n(p) = \frac{p y_n(p)}{\int_0^\infty p y_n(p)\,dp} \tag{2}$$

In Eq. (1), $x_0(p)$ represents the distribution function of the overhead product. Similarly, for the stripping section,

$$y_s^*(p) = \frac{R^*}{R^*+1}\,x^*_{s+1}(p) - \frac{x_0^*(p)}{R^*-1} \tag{3}$$

and

$$x_s^*(p) = \frac{p y_s^*(p)}{\int_0^\infty p y_s^*(p)\,dp} \tag{4}$$

where now $y^*_s(p)$ and $x_s^*(p)$ are, respectively, the

* Department of Chemistry and Chemical Engineering, University of California, Berkeley, California.
** On leave at Department of Chemical Engineering, Cambridge University, England.

distribution functions of the vapour stream and the liquid stream leaving the sth plate, R^* is the reflux ratio in the stripping section, and $x_0^*(p)$ is the distribution function of the bottom product. It has been assumed also, for simplicity, that the relative volatility of every component is the same in both sections of the column, but this is not at all necessary.

Equations (1) and (2) are the basic equations and in Part I it was shown that the composition on any plate is given by

$$x_n(p) = \frac{\dfrac{px_0(p)}{R}\, P\displaystyle\int_0^\infty \frac{\lambda^{n-1}\,C(\lambda)}{\lambda - p}\,d\lambda + \frac{p^{n-2}C(p)}{x_0(p)}\,w(p)}{\displaystyle\int_0^\infty \lambda^{n-1}\,C(\lambda)\,d\lambda} \tag{5}$$

where the symbol P in front of an improper integral denotes its Cauchy principal value, that is

$$P\int_0^\infty \frac{f(\lambda)}{\lambda - p}\,d\lambda \equiv \lim_{\epsilon \to 0}\left[\int_0^{p-\epsilon} \frac{f(\lambda)}{\lambda - p}\,d\lambda + \int_{p+\epsilon}^\infty \frac{f(\lambda)}{\lambda - p}\,d\lambda\right] \tag{6}$$

Also,

$$C(\lambda) \equiv \frac{\lambda\, x_0(\lambda)}{[w(\lambda)]^2 + [\pi\lambda\, x_0(\lambda)]^2} \tag{7}$$

and

$$w(\lambda) \equiv R - P\int_0^\infty \frac{q\, x_0(q)}{\lambda - q}\,dq \tag{8}$$

Eq. (5) then expresses the functional dependence of $x_n(p)$ on both p and n in a closed form. It enables one to calculate $x_n(p)$ directly, that is without making use of any intermediate steps, if the distribution function of the overhead product, $x_0(p)$ is known. Moreover, it can easily be shown [1] that Eq. (5) reduces to FENSKE's well-known equation as $R \to \infty$

Eq. (5) can, however, be put into a more convenient form by introducing a new function, $G(\lambda)$, defined as,

$$G(\lambda) \equiv \frac{C(\lambda)}{C(h)}\left(\frac{\lambda}{h}\right)^{N-1} \tag{9}$$

where $n = N$ denotes the feed plate and h is some point on the p-axis which is, as yet, arbitrary. Then, at the feed plate

$$x_N(p) = \frac{px_0(p)}{R}\,\frac{P\displaystyle\int_0^\infty \frac{G(\lambda)}{\lambda - p}\,d\lambda + \frac{G(p)}{px_0(p)}\,w(p)}{\displaystyle\int_0^\infty G(\lambda)\,d\lambda} \tag{10}$$

A useful asymptotic expression can be obtained from the above, since, when $x_0(p)$, for a given value of p, is small enough that

$$p\,x_0(p)\,P\int_0^\infty \frac{G(\lambda)}{\lambda - p}\,d\lambda \ll G(p)\,w(p) \tag{11}$$

then

$$x_N(p) \to \frac{G(p)\,w(p)}{R\displaystyle\int_0^\infty G(\lambda)\,d\lambda} \tag{12}$$

Finally, the point h should be chosen in such a way as to facilitate the numerical evaluation of the formulae. In other words, h should be chosen so that

$$G(p) \ll 1 \qquad \text{for } p \ll h$$

and

$$G(p) < 10 \qquad \text{for } p > h$$

Entirely analogous formulae are obtained for the stripping section. It is found that

$$x_s^*(p) = \frac{\dfrac{px_0^*(p)}{R^*}\, P\displaystyle\int_0^\infty \frac{\lambda^{-s-1}C^*(\lambda)}{p - \lambda}\,d\lambda + \frac{p^{-s-1}C^*(p)}{px_0^*(p)}\,w^*(p)}{\displaystyle\int_0^\infty \lambda^{-s-1}C^*(\lambda)\,d\lambda} \tag{13}$$

where $C^*(\lambda)$ and $w^*(\lambda)$ are defined by expressions analogous to equations (7) and (8), respectively, that is

$$C^*(\lambda) \equiv \frac{\lambda\, x_0^*(\lambda)}{[w^*(\lambda)]^2 + [\pi\lambda\, x_0^*(\lambda)]^2} \tag{14}$$

and

$$w^*(\lambda) \equiv R^* - P\int_0^\infty \frac{q\, x_0^*(q)}{q - \lambda}\,dq \tag{15}$$

VOL. 4 1955

Again, in order to facilitate the numerical work, define

$$G^*(\lambda) \equiv \frac{C^*(\lambda)}{C^*(l)} \left(\frac{l}{\lambda}\right)^{S+1} \tag{16}$$

where the symbol $s = S$ denotes the feed tray and l is somewhat arbitrary but must be chosen properly. Then

$$x_S^*(p) = \frac{P\int_0^\infty \frac{G^*(\lambda)}{p-\lambda}\,d\lambda + \frac{G^*(p)}{p x_2^*(p)}\,w^*(p)}{\frac{p x_0^*(p)}{R^*}\int_0^\infty G^*(\lambda)\,d\lambda} \tag{17}$$

and if $x_0^*(p)$ is small enough

$$x_S^*(p) \to \frac{G^*(p)\,w^*(p)}{R^*\int_0^\infty G^*(\lambda)\,d\lambda} \tag{18}$$

Moreover, at the feed plate

$$x_S^*(p) = x_N(p)$$

and therefore

$$\frac{x_0(p)}{x_0^*(p)} = \frac{ZR}{R^*}\,\frac{P\int_0^\infty \frac{G^*(\lambda)}{p-\lambda}\,d\lambda + \frac{G^*(p)}{p\,x^*{}_0(p)}\,w^*(p)}{P\int_0^\infty \frac{G(\lambda)}{\lambda-p}\,d\lambda + \frac{G(p)}{p\,x_0(p)}\,w(p)} \tag{19}$$

where

$$Z \equiv \frac{\int_0^\infty G(\lambda)\,d\lambda}{\int_0^\infty G^*(\lambda)\,d\lambda} \tag{20}$$

If either $x_0^*(p)$ or $x_0(p)$ is small, then Eq. (19) can be simplified to give, respectively,

$$G^*(p) = \frac{R^*\,p\,x_0(p)}{ZR\,w^*(p)}\left[P\int_0^\infty \frac{G(\lambda)}{\lambda-p}\,d\lambda + \frac{G(p)}{p\,x_0(p)}\,w(p)\right] \tag{21}$$

and

$$G(p) = \frac{RZ\,p\,x_0^*(p)}{R^*w(p)}\left[P\int_0^\infty \frac{G^*(\lambda)}{p-\lambda}\,d\lambda + \frac{G^*(p)}{p\,x_0^*(p)}\,w^*(p)\right] \tag{22}$$

The Numerical Evaluation of an Improper Integral

Since all the important formulae of the preceding section included the Cauchy principal value of an improper integral, it was thought that a method should be presented here for numerically calculating such a function. Let us suppose then that $f(x)$ is a single-valued, integrable, continuous function of x, which vanishes everywhere for negative x. Then

$$I(\lambda) \equiv \int_0^\infty \frac{f(x)}{\lambda - x}\,dx = \int_{+0}^\infty \frac{f(\lambda-x) - f(\lambda+x)}{x}\,dx \tag{23}$$

or

$$I(\lambda) = \int_{+0}^\infty \phi\,(\lambda, x)\,dx \tag{24}$$

The above integral can now be evaluated numerically in a number of ways, but use will be made here of Simpson's rule, that is, if the x-axis is subdivided into m equal intervals of length h, where m is even, then according to Simpson's formula

$$I(\lambda) = \frac{2h}{3}\left[\frac{\phi\,(\lambda, 0)}{2} + 2\sum_1^{m/2} \phi\,(\lambda, 2kh - h) + \sum_1^{m/2-1} \phi\,(\lambda, 2kh) + \frac{\phi\,(\lambda, mh)}{2}\right] \tag{25}$$

The various ordinates can, of course, be easily evaluated numerically except for $\phi\,(\lambda, 0)$. However,

$$\phi(\lambda,0) = \lim_{x\to 0} \frac{f(\lambda-x) - f(\lambda+x)}{x} = -2f'(\lambda) \tag{26}$$

A convenient method for obtaining the derivative of a function has been described by Rutledge [2], and below are two of his results :

(a) If, for $x - 2h \leqq q \leqq x + 2h$, $f(q)$ can be represented as a polynomial of the fourth degree, then

$$f'(q) = \frac{1}{12h}\left[f(x-2h) - f(x+2h) + 8\{f(x+h) - f(x-h)\}\right] \quad (27)$$

(b) If, for $x - 3h \leq q \leq x + 3h$, $f(q)$ can be represented as a polynomial of the sixth degree, then

$$f'(q) = \frac{1}{180h}\Big\{3\left[f(x+3h) - f(x-3h)\right] + 27\left[f(x-2h) - f(x+2h)\right] + 135\left[f(x+h) - f(x-h)\right]\Big\} \quad (28)$$

Finally, define

$$z(\lambda, kh) \equiv \frac{f(\lambda - kh) - f(\lambda + kh)}{k} \quad (29)$$

Table 1. *Numerical values for* $p\,x_F(p) = 2{\cdot}25676\,p\,(p-1)^2\,e^{-(p-1)^2}$.

p	$p\,x_F(p)$	p	$p\,x_F(p)$	p	$p\,x_F(p)$
1·00	0·00000	2·35	1·56215	3·70	0·04153
1·05	0·00591	2·40	1·49534	3·75	0·03325
1·10	0·02458	2·45	1·41999	3·80	0·02648
1·15	0·05709	2·50	1·33798	3·85	0·02095
1·20	0·10408	2·55	1·25112	3·90	0·01649
1·25	0·16563	2·60	1·16120	3·95	0·01286
1·30	0·24132	2·65	1·06988	4·00	0·01003
1·35	0·33019	2·70	0·97867	4·05	0·00776
1·40	0·43077	2·75	0·88894	4·10	0·00596
1·45	0·54117	2·80	0·80182	4·15	0·00456
1·50	0·65909	2·85	0·71830	4·20	0·00347
1·55	0·78193	2·90	0·63913	4·25	0·00261
1·60	0·90691	2·95	0·56490	4·30	0·00197
1·65	1·03112	3·00	0·49601	4·35	0·00147
1·70	1·15167	3·05	0·43268	4·40	0·00110
1·75	1·26579	3·10	0·37502	4·45	0·00081
1·80	1·37086	3·15	0·32327	4·50	0·00060
1·85	1·46460	3·20	0·27637	4·55	0·00043
1·90	1·54507	3·25	0·23503	4·60	0·00032
1·95	1·61073	3·30	0·19863	4·65	0·00023
2·00	1·66043	3·35	0·16683	4·70	0·00016
2·05	1·69361	3·40	0·13927	4·75	0·00012
2·10	1·71001	3·45	0·11556	4·80	0·00008
2·15	1·70989	3·50	0·09530	4·85	0·00006
2·20	1·69391	3·55	0·07813	4·90	0·00004
2·25	1·66306	3·60	0·06367	4·95	0·00003
2·30	1·61862	3·65	0·05158	5·00	0·00002

Then

$$I(\lambda) = \frac{2}{3}\left[-hf'(\lambda) + 2\sum_{1}^{m/2} z(\lambda, 2kh - h) + \sum_{1}^{m/2-1} z(\lambda, 2kh) + \frac{z(\lambda, mh)}{2}\right] \quad (30)$$

The above is believed to be the simplest form into which Eq. (23) can be reduced.

A Numerical Example

Let $x_F(p)$, the distribution function of the feed, be given by

$$x_F(p) = \frac{4}{\sqrt{\pi}}(p-1)^2\,e^{-(p-1)^2} \quad \text{for all } p > 1 \quad (31)$$

and $x_F(p) = 0$ for $p < 1$. The vapour to liquid ratio in the feed is equal to 1. Moreover, it is specified that

$$x_0(1{\cdot}50)/x_0^*(1{\cdot}50) = 20{\cdot}0$$
$$x^*_0(2{\cdot}95)/x_0(2{\cdot}95) = 20{\cdot}0 \quad (32)$$

and that $R = 2{\cdot}15$. Tables 1 and 2 show some numerical results.

It is found from the calculations that

$$D = 0{\cdot}50913,\ RD = 1{\cdot}09463 \text{ and } R^*W = 1{\cdot}59462$$

Table 2. *A preliminary estimate of the functions* $\lambda\,Dx_0(\lambda)$ *and* $\lambda W x_0^*(\lambda)$.

λ	$Dx_0(\lambda)$	$\lambda W x_0^*(\lambda)$	λ	$\lambda Dx_0(\lambda)$	$\lambda W x_0^*(\lambda)$
1·45	0·53767	0·00350	2·30	0·60392	1·01470
1·50	0·62343	0·03566	2·35	0·53824	1·02391
1·55	0·70390	0·07803	2·40	0·47316	1·02218
1·60	0·77772	0·12919	2·45	0·41089	1·00911
1·65	0·84281	0·18832	2·50	0·35162	0·98636
1·70	0·89593	0·25574	2·55	0·29644	0·95468
1·75	0·93608	0·32971	2·60	0·24562	0·91558
1·80	0·96318	0·40768	2·65	0·20022	0·86965
1·85	0·97624	0·48836	2·70	0·15949	0·81918
1·90	0·97454	0·57053	2·75	0·12386	0·76508
1·95	0·95993	0·65080	2·80	0·09312	0·70870
2·00	0·93304	0·72739	2·85	0·06714	0·65116
2·05	0·89497	0·79864	2·90	0·04495	0·59419
2·10	0·84776	0·86225	2·95	0·02753	0·53737
2·15	0·79339	0·91650	3·00	0·01550	0·49290
2·20	0·73318	0·96073	3·05	0·00420	0·42848
2·25	0·66952	0·99355			

Table 3 (*a*)

λ	$w^*(\lambda)$	$\lambda W x_0^*(\lambda)$	$C^*(\lambda)$	λ	$w^*(\lambda)$	$\lambda W x^*_0(\lambda)$	$C^*(\lambda)$
1·45625	0·01359	0·00696	103·61296	1·55625	− 0·29922	0·08400	5·20845
1·4625	− 0·01078	0·01058	85·50896	1·56250	− 0·31607	0·09007	4·93945
1·46875	− 0·03448	0·01436	43·95479	1·56875	− 0·33258	0·09628	4·70195
1·4750	− 0·05752	0·01830	27·30912	1·5750	− 0·34873	0·10262	4·49048
1·48125	− 0·07989	0·02240	19·50499	1·58125	− 0·36453	0·10907	4·30086
1·4875	− 0·10160	0·02666	15·17744	1·5875	− 0·37998	0·11565	4·12974
1·49375	− 0·12264	0·03108	12·48312	1·59375	− 0·39508	0·12236	3·97437
1·500	− 0·14301	0·03566	10·66428	1·600	− 0·40983	0·12919	3·83259
1·50625	− 0·16100	0·04048	9·49112	1·60625	− 0·42413	0·13613	3·70342
1·51250	− 0·17881	0·4543	8·36595	1·6125	− 0·43811	0·14319	3·58413
1·51875	− 0·19645	0·05052	7·81731	1·61875	− 0·45177	0·15039	3·47351
1·5250	− 0·21391	0·05575	7·19858	1·6250	− 0·46510	0·15772	3·37055
1·53125	− 0·23120	0·06111	6·67832	1·63125	− 0·47830	0·16517	3·27328
1·53750	− 0·24832	0·06661	6·23433	1·63750	− 0·49096	0·17276	3·18346
1·54375	− 0·26526	0·07225	5·85068	1·64375	− 0·50327	0·18047	3·09915
1·5500	− 0·28202	0 07803	5·51555	1·6500	− 0·51524	0·18832	3·01980

Table 3 (b)

λ	$w(\lambda)$	$\lambda D x_0(\lambda)$	$C(\lambda)$	λ	$w(\lambda)$	$\lambda D x_0(\lambda)$	$C(\lambda)$
2·8125	− 0·34350	0·08627	4·44756	2·9375	− 0·13811	0·03161	10·78167
2·825	− 0·32334	0·07966	4·70278	2·950	− 0·11777	0·02753	12·72591
2·8375	− 0·30312	0·07328	4·99194	2·9625	− 0·09940	0·02445	15·29186
2·850	− 0·28284	0·06714	5·32286	2·975	− 0·08027	0·02142	19·26582
2·8625	− 0·26256	0·06115	5·70190	2·9875	− 0·06037	0·01844	25·99771
2·875	− 0·24218	0·05545	6·14927	3·00	− 0·03971	0·01550	38·75103
2·8875	− 0·22169	0·05005	6·68687	3·0125	− 0·01637	0·01261	67·74756
2·90	− 0·20111	0·04495	7·34649	3·025	0·00646	0·00976	98·11714
2·9125	− 0·17978	0·04032	8·22783	3·0375	0·02878	0·00696	52·58279
2·925	− 0·15878	0·03588	9·33889				

Table 4 (*a*). *Numerical values for* $G(\lambda)$. $N = 36$ *and* $S = 54$

λ	$G(\lambda)$	λ	$G(\lambda)$	λ	$G(\lambda)$	λ	$G(\lambda)$
2·70	0·01082	2·8375	0·10059	2·975	2·10394	3·1125	0·95156
2·7125	0·01476	2·850	0·12510	2·9875	3·34344	3·125	0·82655
2·725	0·01820	2·8625	0·15619	3·00	5·86495	3·1375	0·72609
2·7375	0·02119	2·875	0·19619	3·0125	12·05879	3·150	0·64354
2·750	0·02380	2·8875	0·24833	3·025	20·52533	3·1625	0·57682
2·7625	0·03273	2·90	0·31735	3·0375	12·91910	3·175	0·51931
2·775	0·04037	2·9125	0·41317	3·050	3·47029	3·1875	0·46889
2·7875	0·04743	2·925	0·51768	3·0625	2·29453	3·20	0·42494
2·80	0·05338	2·9375	0·73023	3·075	1·70332	3·30	0·21647
2·8125	0·06575	2·950	1·00000	3·0875	1·34813	3·40	0·12006
2·825	0·08120	2·9625	1·41732	3·100	1·11177		

Table 4 (b). Numerical values for $G^*(\lambda)$. $N = 36$ and $S = 54$

λ	$G^*(\lambda)$	λ	$G^*(\lambda)$	λ	$G^*(\lambda)$	λ	$G^*(\lambda$
1·200	0·16677	1·425	3·64364	1·5125	0·50895	1·5875	0·01713
1·250	0·30875	1·4375	6·00723	1·51875	0·37006	1·59375	0·01328
1·300	0·54662	1·45	13·76852	1·525	0·27198	1·600	0·01033
1·3125	0·63335	1·45625	49·49106	1·53125	0·20145	1·60625	0·00805
1·325	0·73229	1·4625	32·27127	1·5375	0·15033	1·6125	0·00629
1·3375	0·84708	1·46875	13·12046	1·54375	0·11295	1·68175	0·00493
1·350	0·98126	1·475	6·45393	1·550	0·08519	1·625	0·00387
1·3625	1·15219	1·48125	3·65310	1·55625	0·06449	1·63125	0·00304
1·375	1·36671	1·4875	2·25500	1·5625	0·04905	1·6375	0·00240
1·3875	1·64204	1·49375	1·47272	1·56875	0·03749	1·64375	0·00189
1·400	2·01011	1·500	1·0000	1·5750	0·02877	1·6500	0·00150
1·4125	2·60980	1·50625	0·70802	1·58125	0·02216		

Next, choose $h = 2{\cdot}95$ and $l = 1{\cdot}50$ and calculate the functions $w(\lambda)$, $C(\lambda)$, $G(\lambda)$, $w^*(\lambda)$, $C^*(\lambda)$ and $G^*(\lambda)$. It was found by repeated trial and error that letting $N = 36$ and $S = 54$ was fairly satisfactory. Many of the values shown in Tables 3 (a) and 3 (b) were obtained by a parabolic interpolation. The values of $G(\lambda)$ and $G^*(\lambda)$, shown in Tables 4 (a) and 4 (b) were either calculated from Eq. (9), $2{\cdot}70 \leqq \lambda \leqq 3{\cdot}0375$, and Eq. (16), $1{\cdot}45624 \leqq \lambda \leqq 1{\cdot}6500$, respectively, or from Eq. (22), $\lambda > 3{\cdot}05$, and Eq. (21), $\lambda \leqq 1{\cdot}450$, respectively. The tabulated values of $G(\lambda)$ and $G^*(\lambda)$ for the latter two ranges, respectively, are only approximately correct. One also finds from Eq. (20) that

$$Z = 0{\cdot}86938$$

Finally, by means of Eq. (19) and the obvious relation

$$x_F(p) = D\,x_0(p) + W x_0^*(p)$$

one calculates numerically the functions $\lambda D\,x_0(\lambda)$ and $\lambda W x_0^*(\lambda)$. The results are presented in Table 5.

Table 5. Calculated numerical values for $\lambda Dx_0(\lambda)$ and $\lambda Wx_0^*(\lambda)$

λ	$\lambda Dx_0(\lambda)$	$\lambda Wx^*_0(\lambda)$	λ	$\lambda Dx_0(\lambda)$	$\lambda Wx_0^*(\lambda)$
1·45	0·53767	0·00350	2·30	0·37281	1·04581
1·50	0·62343	0·03556	2·35	0·30782	1·05433
1·55	0·71266	0·6927	2·40	0·44425	1·05109
1·60	0·78752	0·11939	2·45	0·38299	1·03700
1·65	0·86159	0·17954	2·50	0·32509	1·01289
1·70	0·88949	0·26219	2·55	0·27131	0·97981
1·75	0·92525	0·34054	2·60	0·22202	0·93918
1·80	0·94736	0·42350	2·65	0·17759	0·89229
1·85	0·95564	0·50896	2·70	0·14026	0·83841
1·90	0·95058	0·59449	2·75	0·10781	0·78113
1·95	0·93280	0·67793	2·80	0·08049	0·72133
2·00	0·90327	0·75716	2·85	0·05799	0·66031
2·05	0·86390	0·82971	2·90	0·04042	0·59871
2·10	0·81578	0·89423	2·95	0·02753	0·53737
2·15	0·76080	0·94909	3·00	0·01580	0·48021
2·20	0·70081	0·99310	3·05	0·00420	0·42848
2·25	0·63765	1·02541			

A comparison now between Tables 5 and 2 will reveal that the two functions $\lambda Dx_0(\lambda)$, that is, the one which was assumed, and the one which was calculated, are not very different. The agreement between said two functions however cannot be considered, in this particular problem at least, satisfactory, because, as can be verified by a numerical calculation, a small change in $w(\lambda)$ and $w^*(\lambda)$ will alter the functions $C(\lambda)$ and $C^*(\lambda)$ considerably, especially in the sensitive regions $2{\cdot}95 < \lambda < 3{\cdot}10$ and $1{\cdot}40 < \lambda < 1{\cdot}50$. This is due to the fact that R was deliberately chosen close to $R_{\min}$, and therefore, in this case at any rate, the numerical values of both N and S would markedly depend on the assumed distribution functions of the two products. This of course, would be expected; on the other hand, it is somewhat surprising to find that the functions $C(\lambda)$ and $C^*(\lambda)$, and therefore $G(\lambda)$, $G^*(\lambda)$, N and

VOL. 4 1955

S, do depend in a very pronounced manner on the assumed values of the distribution function for $2{\cdot}95 < \lambda < 3{\cdot}05$ and $1{\cdot}45 < \lambda < 1{\cdot}50$, respectively. It is true that $\lambda D x_0(\lambda)$ is small for $2{\cdot}95 < \lambda < 3{\cdot}05$, yet it is precisely the value of $\lambda D x_0(\lambda)$ in the above mentioned interval which, together with $w(\lambda)$, primarily determines the function $G(\lambda)$; entirely analogous considerations can be made concerning $\lambda W x_0^*(\lambda)$ for $1{\cdot}45 < \lambda < 1{\cdot}50$. We see then that $G(\lambda)$, which is large only for $3{\cdot}05 > \lambda > 2{\cdot}95$, depends markedly on the whole distribution function $D x_0(\lambda)$, and not only on part of it, as one would have expected. So, one of the difficulties which one encounters in such problems is to be able to estimate the distribution functions of the products in every detail. That is even in the regions where they come numerically very small. And it is because this estimate of the distribution functions can be made more rapidly that the analytic form of the solution is preferable to that obtained by the iterative method. Moreover, by means of the analytic solution, one can see more clearly, than by the iterative solution, which factors in any numerical problem primarily affect the answer and to what an extent.

This numerical example, then was presented in order to illustrate the application of the formulae to an actual problem, to point out certain of the difficulties encountered in such problems, and to bring out certain of the characteristic features of the analytic solution which should make it superior to that derived by the iterative method. In order to solve this problem completely one should revise the original estimate on the function $\lambda D x_0(\lambda)$ and repeat the procedure outlined in this chapter, until the assumed and the calculated values for $\lambda D x_0(\lambda)$ become essentially identical; this, however, shall not be attempted here.

The Plate by Plate Method

In Part I it was shown that the composition of the liquid on any tray is given by

$$x_n = \frac{x_0 X_n}{\int_0^\infty x_0 X_n \, dp}$$

where

$$\underset{n+1}{X}(p) = R\, p\, X_n(p) + p \int_0^\infty x_0(p)\, X_n(p)\, dp$$

with

$$X_1(p) = \frac{p}{R}$$

Successive substitutions will show that if M_s is defined by

$$M_s = \int_0^\infty x_0(p)\, p^s \, dp$$

then

$$X_2(p) = p^2 + \frac{p}{R} M_1$$

$$X_3(p) = R p^3 + p^2 M_1 + p\left(M_2 + \frac{1}{R} M_1^2\right)$$

and, in general

$$X_n(p) = P_n(p)$$

where $P_n(p)$ is a polynomial of the nth degree having only positive coefficients. Therefore $P_n(p)$ is positive and strictly monotone increasing. Further

$$x_n = \frac{P_n}{N_n} x_0$$

with

$$N_n = \int_0^\infty x_0(p)\, P_n(p)\, dp$$

X_n has a form independent of the distribution function and the same may be said for N_n. Also the coefficients in P_n depend only upon the reflux ratio and the successive statistical moments of the distribution function. The method of calculating the composition on a particular plate, knowing the composition of the overhead is then a straightforward task on a modern computing machine. A programme for doing this has been prepared for the I.B.M. 602 A.

Conclusions

The solution just outlined to the basic equation for the rectification of complex mixtures in an ideal plate column has all the well-known attractive features of an expression in a closed form. At this point, however, one might be

tempted to ask whether or not it would have been simpler to break up the complex mixture into a finite number of distinguishable components and then make use of the equations already developed by UNDERWOOD and the other investigators, rather than employ the formulae of this paper. On the contrary, it would be preferable, in general, to replace a large number of distinguishable components b ya continuum, because the expressions developed here are easier to handle than the corresponding ones for the finite problem. For, it will be remembered that in UNDERWOOD's method one has to calculate by trial and error some of the roots of the equation

$$\sum_{j=1}^{m} \frac{p(j)\, x_0(j)}{\lambda - p(j)} = R$$

where m is the total number of components in the mixture, whereas in the method just outlined no such trial and error calculation is necessary. And at any rate, the expressions presented in this paper can be easily evaluated numerically by means of a digital computer, a feature which should add, naturally, to the usefulness of this analytic solution.

NOTATION

$x_n(i)$ = mole fraction of the ith component in the liquid stream leaving the nth plate in the column

$y_n(i)$ = mole fraction of the ith component in the vapour stream leaving the nth plate in the column

$p \equiv 1/\alpha$ = the reciprocal of the relative volatility

$x_n(p)$ = the distribution function of the liquid stream leaving the nth plate

$y_n(p)$ = the distribution function of the vapour stream leaving the nth plate

$x_0(p)$ = the distribution function of the overhead product

$C(\lambda)$, $w(\lambda)$, and $G(\lambda)$ are functions defined, respectively, by Eqs. (7), (8) and (9).

$P\int_0^\infty \frac{f(x)}{\lambda - x}\, dx$ is the Cauchy principal value of the improper integral

REFERENCES

[1] ACRIVOS, A.; Ph.D. Thesis, University of Minnesota, 1954.

[2] RUTLEDGE, G.; *Phys. Rev.* 1932 **40** 262.

VOL. 4 1955